CAL LAB

THE INTERNATIONAL JOURNAL OF METROLOGY

METROLOGY 101: CALIBRATING DC SHUNTS

2012
JULY
AUGUST
SEPTEMBER

Quality of Air Speed Calibrations

Learning to Apply Metrology Principles to the Measurement of X-ray Intensities in the 500 eV to 110 keV Energy Range

Better accuracy for a broader workload

The 52120A Transconductance Amplifier lets you accurately test and calibrate a broad workload at full current range

The 52120A expands your calibration capabilities to a broad workload of power and energy meters, clamp meters, CTs and Rogowski coils—up to 6000 A. Use it with all Fluke Calibration calibrators, including the 5080A, 9100, 55XX and 57XX Series. For enhanced accuracy, use it closed-loop with the 610X Electrical Power Standards.

- Output ranges: 2 A, 20 A, 120 A
- Frequency to 10 kHz
- Generate 3,000 or 6,000 amps with accessory coils
- Industry-leading amplifier accuracy

Get the details: **www.flukecal.com/52120A**

Fluke Calibration. *Precision, performance, confidence.*™

Electrical	RF	Temperature	Pressure	Flow	Software

FLUKE ® Calibration

CAL LAB
THE INTERNATIONAL JOURNAL OF METROLOGY

VOLUME 19, NUMBER 3

www.callabmag.com

FEATURES

DEPARTMENTS

ON THE COVER: Paula Heath calibrates pipettes at Calibrate, Inc. in Carrboro, NC. Using the gravimetric method, she is testing this instrument for accuracy and precision after calibration adjustment. Calibrate founded the on-site pipette calibration industry twenty-nine years ago in St. Louis, MO and specializes in helping labs maintain compliance in regulatory environments.

CALENDAR

CONFERENCES & MEETINGS 2012

Jul 26 NACLA Annual General Meeting (AGM). Sacramento, CA. The NACLA AGM will be begin at approximately 8:30 am on Thursday, July 26, 2012 at the Sheraton Grand Sacramento Hotel, in cooperation with the NCSLI Conference. For questions or details contact ruttenweiler@nacla.net or visit http://www.nacla.net.

Jul 29-Aug 3 NCSL International. Sacramento, CA. This year's theme is "The Business End of Metrology Quality and Testing." http://www.ncsli.org.

Jul 29 Fluke Calibration Software User Group Meeting at NCSLI. Sacramento, CA. Meets Sunday 9:00 am to 3:00 pm. Register online at http://us.flukecal.com/ncsli.

Sep 9-14 XX IMEKO World Congress. Busan, Republic of Korea. Hosted by the Korea Reaseach Institute of Standards and Science (KRISS), this year's theme for the International Measurement Confederation is "Metrology for Green Growth ." http://imeko2012.kriss.re.kr/.

Sep 10-13 AUTOTESTCON 2012. Anaheim, CA. Sponsored annually by the IEEE, the theme this year is "Mission Assurance through Advanced ATE." http://autotestcon.com.

Sep 18-19 The Energy and Low Carbon Technology Conference 2012. London, England. The theme is "Measurement Makes Business Sense." For further information, please visit: http://www.tuvnel.com/tuvnel/energy_and_low_carbon_technology_conference.

Oct 8-12 Simposio de Metrología 2012. Santiago de Querétaro, Mexico. This year's slogan is "Innovation in measurements for a better quality of life." Hosted by the National Institute of Metrology of Mexico, Centro Nacional de Metrología, CENAM, http://www.cenam.mx/simposio/.

Oct 21-26 ASPE Annual Meeting. San Diego, CA. The 27th American Society for Precision Engineering Annual Meeting will provide a forum for presentation and discussion of the latest technical information and achievements in precision engineering. http://aspe.net/.

Nov 2-4 India Lab Expo 2012. Hyderbad, India. The 4th International Indian exhibition is a lead national & international meeting point for decision-makers and experts from all related to scientific & laboratory industries. http://www.indialabexpo.com.

CAL LAB
THE INTERNATIONAL JOURNAL OF METROLOGY

PUBLISHER'S LOG

Accuracy vs. Peace on Earth

The other night, my wife, Sita, and I had a spirited disagreement over the accuracy of her method of measuring the length of the living room. Not wanting to go downstairs to track down a measuring tape, she laid down on the floor four times, using a cat toy to mark where her feet/head landed on the floor. She ignored my protests of how inaccurate her method was, considering the variables: she is 5 feet and one half of an inch tall and the cat toy is about two inches wide. Well, after I got the measuring tape, turns out she was just an inch and a half off of her measurement of 20 feet—error rate of 0.625%±. I'm all for thinking outside the box and using whatever you have at your disposal to answer a nagging question, but when it comes to measurement, I couldn't shake the mindset of a metrologist… her method just rubbed me the wrong way and made my hackles stand up. But, I had to give her kudos for her results, for the sake of Peace on Earth.

I have been in this industry for 15 years, and I know if we added a resolution contributor of ±1 Sita, we could see just how uncertain I am about her methodology. But what I do love about metrology is how it affects everything; I can relate my career as a metrologist to just about every profession. The diversity is amazing… just look at the papers we have in this issue.

Most people associate X-rays with a broken bone or two, but few know just what it takes to peer under the skin using yet another technology that needs metrology. In this issue, we have "Learning to Apply Metrology Principles to the Measurement of X-ray Intensities in the 500 eV to 110 keV Energy Range," a paper contributed by National Security Technologies LLC.

Rachael Coquilla, President of Bryza Wind Lab in Fairfield, California, contributed her article on the "Quality of Air Speed Calibrations," focused on qualifying wind tunnels for wind sensor calibration testing. It only takes a little wind tunnel metrology to affect the design and engineering of everything from buildings to jet planes.

And for this issue's Metrology 101 article, Jay Klevens of Ohm-Labs, contributed his expertise on "Calibrating DC Shunts: Techniques and Uncertainties." This article may be a little advanced for a Metrology 101, but current shunt calibration is not simple. With today's industry and the push towards 17025 and Z540.3, understanding the contributors to our uncertainties is crucial to our measurements.

I hope to see all of you at the NCSLI Conference in Sacramento, California—booth 623—or upstairs at AUTOTESTCON in Anaheim, so be sure to stop by and lets us know how we are doing and what you would like to see in the magazine.

Live Long and Measure,

Mike Schwartz

CALENDAR

SEMINARS: Online & Independent Study

ASQ CCT (Certified Calibration Technician) Exam Preparation Program. Learning Measure. http://www.learningmeasure.com/.

AC-DC Metrology– Self-Paced Online Training. Fluke Training. http://us.flukecal.com/training/courses.

Basic Measurement Concepts Program. Learning Measure. http://www.learningmeasure.com/.

Basic Measuring Tools – Self Directed Learning. The QC Group, http://www.qcgroup.com/calendar/.

Basic RF and Microwave Program. Learning Measure. http://www.learningmeasure.com/.

Introduction to Measurement and Calibration – Online Training. The QC Group, http://www.qcgroup.com/calendar/.

Intro to Measurement and Calibration – Self-Paced Online Training. Fluke Training. http://us.flukecal.com/training/courses.

ISO/IEC 17025 Compliance. Workplace Training, tel (612) 308-2202, info@wptraining.com, http://www.wptraining.com/.

Measurement Uncertainty – Self-Paced Online Training. Fluke Training. http://us.flukecal.com/training/courses.

Measurement Uncertainty Analysis – Online Training. The QC Group, http://www.qcgroup.com/calendar/.

Metrology for Cal Lab Personnel– Self-Paced Online Training. Fluke Training. http://us.flukecal.com/training/courses.

Metrology Concepts. QUAMETEC Institute of Measurement Technology. http://www.QIMTonline.com.

Precision Dimensional Measurement – Online Training. The QC Group, http://www.qcgroup.com/calendar/.

Precision Measurement Series Level 1. Workplace Training, tel (612) 308-2202, info@wptraining.com, http://www.wptraining.com/.

Precision Electrical Measurement – Self-Paced Online Training. Fluke Training. http://us.flukecal.com/training/courses.

Precision Measurement Series Level 1. Workplace Training, tel (612) 308-2202, info@wptraining.com, http://www.wptraining.com/.

Magnetic Field Measurement

Fluxgate Transducers

Bartington® Instruments

High Sensitivity for Low Fields

One and Three-axis Transducers with ±10V (±3V Mag640) analog outputs for each axis. For environmental field monitoring, mapping and active cancellation. Cryogenic sensors available.

Field Ranges	70, 100, 250, 500, 1000µT
Frequency Response	dc to 3kHz (-3dB) (Mag03), dc to >1kHz (Mag690, Mag649)
Noise Level	< 12pTrms/√Hz at 1Hz (Mag03 standard), < 6pTrms/√Hz at 1Hz (Mag03 low noise), < 20pTrms/√Hz at 1Hz (Mag690), < 10pTrms/√Hz at 1Hz (Mag649)


Mag648/649


Mag690


Mag-03MS


Mag-03MC

Hall Transducers

Analog Output for Mapping or Control

One-, Two- and Three-axis Transducers with ±10V analog outputs for each axis.

Field Ranges	20mT, 200mT, 2T, 5T, 10T, 20T
Accuracy	±1% or ±0.1%
Frequency Response	dc to 2.5kHz (-3dB); Special to 25kHz
White Noise at >10Hz	0.12µT/√Hz for 2T range (Y-axis), 2µT/√Hz for 2T range (3-axis)

Hall Transducer Probe Packages

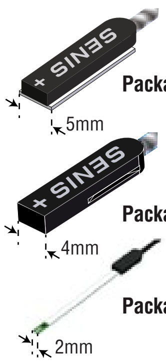

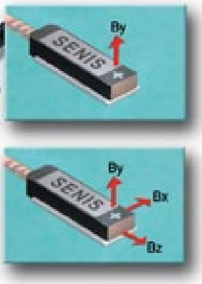

SENIS

USB/Handheld Teslameters

Metrolab

USB Connector, 3-Axis, Handheld PDA Available

For pre-installation site surveys for magnetically sensitive equipment. Post-installation surveys of the dc and ac fringe fields of large magnets and magnetic assemblies. Field harmonic measurements over time for non-invasive load and condition monitoring of ac power assemblies like tranformers and motors.

Fluxgate Probe

Field Range	100µT
Noise	5nT p-p, 8 nT RMS (2kSPS, no averaging); 4nT p-p (100x averaging)

Hall Probe

Field Ranges	0.1T, 0.5T, 3T, 20T
Resolution	3mT on 3T range


TFM1186 Fluxgate Probe


THM1176 Hall Probe

NMR Teslameter

Mapping and Calibration Standard

For field calibration, mapping and control with high resolution,very high stability and absolute accuracy.

Field Ranges	from 0.04T to 13.7T
Resolution	±0.1µT or 1Hz (proton sample)
Absolute Accuracy	±5ppm

RS-232C and IEEE-488 Interfaces

Multiprobe NMR arrays for precision mapping of large magnets


PT2025

Metrolab

CALENDAR

Precision Measurement Series Level 2. Workplace Training, http://www.wptraining.com/.

Vibration and Shock Testing. Equipment Reliability Institute, http://www.equipment-reliability.com/distance_learning.html.

SEMINARS: Dimensional

Aug 9-10 Hands-On Gage Calibration and Repair Workshop. Yorba Linda/Orange County, CA. http://www.iicttraining.com.

Sep 11-12 Hands-On Gage Calibration and Repair Workshop. Schaumburg, IL. http://www.iicttraining.com.

Sep 13-14 Hands-On Gage Calibration and Repair Workshop. Milwaukee, IL. http://www.iicttraining.com.

Sep 26-27 Hands-On Gage Calibration and Repair Workshop. Atlanta, GA. http://www.iicttraining.com.

Oct 1-2 Hands-On Gage Calibration and Repair Workshop. Denver, CO. http://www.iicttraining.com.

SEMINARS: Electrical

Aug 13-16 MET-301 Advanced Hands-On Metrology. Everett, WA. http://www.flukecal.com/training.

Aug 21-23 MET-302 Introduction to Measurement Uncertainty. Everett, WA. http://www.flukecal.com/training.

Sep 5-7 Instrumentation for Test & Measurement. Las Vegas, NV. http://www.ttiedu.com.

Sep 20-21 Essential Metrology for Engineers and Calibration Technicians. Baltimore, MD. WorkPlace Training, http://wptraining.com/.

SEMINARS: Flow & Pressure

Sep 11-13 Fundamentals of Flow Measurement Training Course. Loveland, CO. Colorado Engineering Experiment Station Inc., www.ceesi.com.

Sep 17-20 Comprehensive Flow Measurement Training Course. Loveland, CO. Colorado Engineering Experiment Station Inc., www.ceesi.com.

CALENDAR

Sep 17-21 Principles of Pressure Calibration. Phoenix, AZ. http://us.flukecal.com/training.

Oct 1-3 Flow Measurement and Calibration. Munich, Germany. TrigasFI GmbH, http://www.trigasfi.de/html/en_seminars.htm.

SEMINARS: General

Aug 20-24 Fundamentals of Metrology. Gaithersburg, MD. Sponsored by NIST Office of Weights and Measures. http://www.nist.gov/pml/wmd/5179.cfm.

Oct 18 (FT-01) Elements of Measurement Techniques. Irvine, CA. Measurement Science Conference (MSC) Fall Tutorial. http://www.msc-conf.com.

SEMINARS: Industry Standards

Jul 31 Basics of Recognition Class. Washington, DC. "A Basic Explanation of the Laboratory Accreditation Process: Making Sense Out of the Confusion," hosted by the National Cooperation for Laboratory Accreditation (NACLA). Special two hour session, 9:00 am – 11:30 am at the Stimson Center, for those who need to understand the basics of conformity assessment in the US. http://www.nacla.net.

Sep 17-19 Cal Lab Management; Beyond 17025 Training. Baltimore, MD. WorkPlace Training, http://wptraining.com/.

Oct 17-19 ISO/IEC Standard 17025. Upper Marlboro, MD. Training for testing and calibration laboratory personnel presented by the International Accreditation Service. http://www.iasonline.org.

Oct 18 (FT-02) Measurement Fundamentals for Training Calibration Personnel to Meet ISO & FDA Requirements. Irvine, CA. Measurement Science Conference (MSC) Fall Tutorial. http://www.msc-conf.com.

SEMINARS: Mass & Weight

Oct 15 - 26 Mass Seminar. Gaithersburg, MD. Two-week, "hands-on" seminar, sponsored by NIST Office of Weights and Measures. http://www.nist.gov/pml/wmd/5192.cfm.

SEMINARS: Measurement Uncertainty

Aug 20-21 Measurement Uncertainty. La Habra, CA. Training for testing and calibration laboratory personnel presented by the International Accreditation Service. http://www.iasonline.org.

Sep 5 Introduction to Measurement Uncertainty. Web Event hosted by Workplace Training. 10 hours elearning prerequisite included. http://www.wptraining.com.

Sep 18-20 Measurement Uncertainty Workshop. Fenton, MI. QUAMETEC Institute of Measurement Technology. http:// www.QIMTonline.com.

Sep 24-26 Measurement Uncertainty Training Course. Loveland, CO. Colorado Engineering Experiment Station Inc., www.ceesi.com.

Oct 18 (FT-03) Measurement Uncertainty. Irvine, CA. Measurement Science Conference (MSC) Fall Tutorial. http://www.msc-conf.com.

Nov 13-15 Measurement Uncertainty Workshop. Fenton, MI. QUAMETEC Institute of Measurement Technology. http:// www.QIMTonline.com.

SEMINARS: Software

Sep 10-14 (MC-205) Calibration Asset Management. Parsippany, NJ. This five-day course on Calibration Asset Management shows you how to use the calibration software database to generate reports for your calibration lab. http://us.flukecal.com/training.

Sep 17-21 MC-206 Basic MET/CAL® Procedure Writing. Parsippany, NJ. http://us.flukecal.com/training.

SEMINARS: Temperature

Aug 21-23 Infrared Temperature Metrology. American Fork, UT. Fluke Calibration, http://us.flukecal.com/training.

Sep 18-19 ITS-90 Fixed-Point Cell Mini-Workshop. NIST Gaithersburg, MD. http://www.nist.gov/pml/div685/sc/index.cfm.

Sep 18-20 Advanced Topics in Temperature Metrology. American Fork, UT. Fluke Calibration, http://us.flukecal.com/training.

Sep 19-20 Selecting and Using Alternative Thermometers Mini-Workshop. NIST Gaithersburg, MD. http://www.nist.gov/pml/div685/sc/index.cfm.

SEMINARS: Vibration

August 15-17 Fundamentals of Random Vibration and Shock Testing, HALT, ESS, HASS (...). Santa Barbara, CA. http://www.equipment-reliability.com.

Sep 11-13 Seismic Protection of Critical Equipment. Acton, MA. http://www.equipment-reliability.com.

Oct 2-4 Seismic Protection of Critical Equipment. Reno, NV. http://www.equipment-reliability.com.

Oct 9-11 Fundamentals of Random Vibration and Shock Testing, HALT, ESS, HASS (...). Santa Clarita, CA. http://www.equipment-reliability.com.

Oct 15-17 Fundamentals of Vibration and Shock Testing with Emphasis on Fixture Design. Sunnyvale, CA. http://www.equipment-reliability.com.

Oct 29-31 Fundamentals of Random Vibration and Shock Testing, HALT, ESS, HASS (...). Detroit, MI. http://www.equipment-reliability.com.

Visit **www.callabmag.com** for upcoming and future events!

New Vacuum Calibration System: Better, Faster, and Cheaper

In the vacuum business, less is more—except when it comes to accuracy. Industries that depend on high-quality, carefully monitored vacuum for sensitive processes such as microchip fabrication, as well as researchers in numerous technology fields, defense R&D work, and academic science, require high-precision sensors calibrated to authoritative standards.

But until recently, getting direct NIST traceability for vacuum gauges has been a time-consuming and relatively expensive process. Calibrating a customer gauge against one of the national primary standards (that is, one of NIST's Ultrasonic Interferometer Manometers, or UIMs) "usually takes about fifty hours of data-acquisition, followed by a couple of days to write a report," says Jay Hendricks, who is in charge of Low Pressure Manometry in PML's Sensor Science Division. "It's all done manually, with a lot of down time required for the system to pressurize and stabilize. The cost is about $5000, with a turnaround time of approximately eight weeks."

That excludes many potential customers without the requisite time or money. Now, however, even small businesses and labs can take advantage of a new, fully automated calibration system devised by Hendricks and colleague Jacob Ricker.

The system calibrates gauges over five orders of magnitude in pressure, from 0.65 Pa to 130,000 Pa. (The pascal, abbreviated Pa, is the SI unit of pressure. Standard atmospheric air pressure is about 101,000 Pa.) "That's the range in which most chemistry and physics goes on," says Ricker. "For example, on the low side it covers plasma etching, chemical vapor deposition, and sputtering. On the high side, it covers airplane or helicopter altimeters and barometric sensors that need to be traceable to NIST."

Measurement uncertainties in the new VCS device range from 0.1% at 13 Pa to 0.04% at 1,300 Pa to 0.01% or better at 130,000 Pa (k=2) "The manometers still have a much lower uncertainty, but at a significantly higher cost," Ricker says. "At those same pressures the UIM delivers 0.023%, 0.0007%, 0.0005% respectively. But this new system is designed for people who may not need all those zeros, or gauges that don't offer a part in 10-6 resolution."

Setting up the new service demanded a great deal of custom software and hardware integration for automated control of flow and pressurization, as well as monitoring and data-collection. But the system's key element is an extremely accurate and stable transfer standard—a set of interconnected components informally called an "igloo" after the enclosure manufacturer. The device is so good that for most common industrial process vacuum-gauges, it eliminates the need to directly test against a primary UIM situated deep in NIST's Advanced Measurement Laboratories.

The latest version of the transfer standard, which has been under development for more than a decade in NIST's Pressure and Vacuum Group, combines two different kinds of low-pressure sensors enclosed in an insulated container the size of a suitcase that maintains a constant temperature within 5 mK.

Inside is a resonance silicon gauge (RSG) that monitors two capacitance diaphragm gauges (CDGs). RSGs are microelectromechanical systems (MEMS) that measure the effect of pressure- induced strain on the resonant frequency of a silicon oscillator. CDGs measure pressure-induced changes in the position of an alloy diaphragm that serves as one plate of a capacitor, and are the workhorse sensors for most high-precision vacuum operations.

That combination, Hendricks says,

brings unique benefits: "CDGs have extremely fine resolution at low pressure. RSGs have outstanding long term drift stability—in the range of 0.01%, which is a factor of 10 better than the CDGs. So to get the best of both, we use an RSG to calibrate the CDGs. And that occurs every time we turn the system on.

"The software does an automatic calibration routine at the beginning of each test. It checks the CDGs against the RSGs, fills to several cardinal pressure points, and then does an on-site self-calibration—all only a few minutes before the system is used."

The result is a dramatic reduction in uncertainty. "Looking at the entire process," Hendricks says, "we get a factor of five improvement in the long term drift uncertainty by this calibration procedure and another factor of 10 from the igloo, so theoretically that's a total factor of 50 improvement."

The new automated calibration system can handle almost any vacuum gauge that has a digital or DC output. That is important in view of the multiplicity of gauge types and the recent trend is toward combination gauges, such as thermocouples paired with piezorestive sensors.

Those features, combined with a factor of five reduction in cost and significantly shorter turnaround time, is expected to increase the number of customers and provide services to a much wider range of users. Many people contributed to development of the VCS system, notably including John Quintavalle and Jeffrey Kelley (software and apparatus fabrication) and collaborators Patrick Abbott, Justin Chow and Douglas Olson. Financial support was provided by Calibration Service Development.

Source: http://www.nist.gov/pml/div685/vacuum_calibration.cfm (May 8, 2012).

New Website to Educate Industry About Alternatives to Mercury Thermometers

As part of a larger effort to reduce the amount of mercury, a potent neurotoxin, in the environment, the National Institute of Standards and Technology (NIST) has launched a new website to help industry scientists and engineers decide the best temperature measurement alternative for their purposes. The website also includes information about myths pertaining to mercury and temperature measurement and how to safely package and recycle mercury-containing products.

NIST stopped providing calibration services for mercury thermometers on March 1, 2011. This was motivated in part by NIST's work with the Environmental Protection Agency to eliminate as many sources of mercury in the environment as possible.

According to Greg Strouse, leader of NIST's temperature, pressure and vacuum programs, mercury thermometers are neither a superior nor a standard method for measuring temperature.

According to NIST researcher Dawn Cross, industrial scientists commonly object to replacing their mercury thermometers because they have grown accustomed to getting the same answer from their mercury thermometers over the years, even if it is less accurate than can be provided by modern digital thermometers.

Cross points out that other thermometers based on the principle of thermal expansion of a fluid, such as alcohol, are not hopelessly inaccurate. In fact, they are as accurate as mercury thermometers and are suitable for some applications that don't require stringent temperature control. For example, alcohol thermometers might be suitable for measuring the temperature of gasoline and other fuels, but they would be unsuitable for monitoring the temperature of vaccines, the viability of which relies on strict control of their temperature.

Visit the website at www.nist.gov/pml/mercury.cfm for more information about how NIST can help your industry find an accurate, nontoxic and environmentally benign alternative to mercury thermometers.

Source: http://www.nist.gov/pml/div685/mercury-061212.cfm.

NIST Goes the Distance for the Olympics

In yet another Olympian feat of measurement, researchers at the National Institute of Standards and Technology (NIST) recently calibrated a tape that will be used to measure out the distance of this summer's Olympic marathon—a distance of 26 miles 385 yards—to 1 part in 1,000.

Measurement is a vital aspect of the Olympic Games. Officials measure the height of jumps, the speed of races, and the mass of weights to determine who wins a medal and who goes home. The marathon is no different. Because of the difficulties in measuring out the distance, the International Association of Athletic Federations (IAAF) only recognized best times and didn't begin awarding world records for marathons until 2004 when a method using a device called a Jones Counter was officially recognized as sufficiently accurate.

Developed by a father-son duo in the early 1970s,* the Jones Counter is a simple geared device that counts the revolutions of a bicycle wheel. To calibrate the device, course measurers lay out a calibrated measuring tape at least 30 meters in length. Once they have determined the number of revolutions that equal that distance—and a couple of successively longer distances—they follow painstaking procedures for laying out the rest of the course. The measurements, which can take hours to complete, will ensure that the shortest distance a runner will run will be at least the required distance and no more than about 40 meters over, corresponding to an error of about 1 part in 1,000.

Chris Blackburn, a physical science technician with NIST's Semiconductor and Dimensional Metrology Division, says this calibration wasn't terribly difficult, but it was a little unusual because the tape that the course measurer wanted calibrated was 100 meters long, 40 meters longer than the NIST "tape tunnel," so they had to do the calibration in sections.


If you're here, OEM cal/repair service is closer than you might think.
You don't need to give up local convenience to enjoy OEM-quality calibration and repair services. Agilent provides a host of local-access options to fit your specific needs. Together with our delivery partner, we service Agilent and non-Agilent products to keep you up and running wherever you are.
That's thinking ahead. That's Agilent.
Local Agilent Repair & Calibration Options
Local Service Centers — Fast pick-up and delivery
Mobile Cal Labs — Our Service Center comes to you
System Uptime — Our System Engineers come to you
Resident Professional — Dedicated Service Center on your site
Agilent Preferred Service Partner
LOCKHEED MARTIN
We never forget who we're working for™
Agilent Advantage Services
Plan for local service and much more
Discover how Agilent can help
www.agilent.com/find/planlocalservice
u.s. 1-800-829-4444 canada: 1-877-894-4414 mexico: 1-800-254-2440
© 2011 Agilent Technologies, Inc.
Agilent Technologies

"The uncertainties associated with our laser interferometer system are very small," says Blackburn. "And by applying the proper tension on the tape to pull it straight and keeping the temperature at 20 °C, plus or minus 15 hundreths of a degree, we achieve uncertainties of 0.00018 meters, which meets or exceeds our customers' requirements in most cases."

Blackburn's group performs about 40 calibrations annually, mostly for the petroleum and measuring tape manufacturing industry. While the effort that goes into each calibration varies depending on several factors, including tape construction and tape length, most can be completed in a few hours.

The IAAF chose David Katz of Finish Line Road Race Technicians, Inc., and his friend and collaborator Hugh Jones to help perform the measurements, and Katz in turn contacted NIST to perform the calibration of the tape that they used to calibrate their Jones Counters. After making the temperature corrections and compensations for the error that NIST found in the tape (13 mm over 100 meters), Katz and Jones found that their measurements of the marathon course disagreed by 1.3 to 2 meters over the entire distance.

Get Olympics fast facts and other measurements related to sports on the NIST website at www.nist.gov/pml/wmd/metric/olympic-facts.cfm.

* www.jonescounter.com/2.html

Source: http://www.nist.gov/public_affairs/tech-beat/#olympics.

Teledyne Technologies to Acquire LeCroy Corporation

Teledyne Technologies Incorporated and LeCroy Corporation jointly announced they have entered into a definitive agreement that provides for the merger of LeCroy Corporation with a wholly-owned subsidiary of Teledyne. Pursuant to the transaction, Teledyne will acquire all of the outstanding common shares of LeCroy for $14.30 per share payable in cash. The aggregate value for the transaction is approximately $291 million, taking into account LeCroy's stock options, stock appreciation rights and net debt as of March 31, 2012. The transaction was unanimously approved by the Boards of Directors of Teledyne and LeCroy. In addition, LeCroy directors and executive officers, including founder Walter LeCroy, have agreed to vote their shares in favor of the transaction.

Founded in 1964 and headquartered in Chestnut Ridge, N.Y., LeCroy is a leading supplier of oscilloscopes, protocol analyzers and signal integrity test solutions with approximately 500 employees worldwide. For its fiscal year ended July 2, 2011, LeCroy had sales of approximately $178.1 million.

Source: http://www.teledyne.com/news/news.asp.

Edison
Mudcats™
Metrology Software

COMPREHENSIVE SOFTWARE FOR TODAY'S METROLOGY CHALLENGES

CALIBRATION TOOLS
- Calibration Data Collection
- Automation and Scripting
- GPIB/RS-232 Automated Data Sheets
- Automatic OOT Detection
- Multi-Channel Data Collection
- Communicate with other Software via COM

ENGINEERING TOOLS
- Specification Tracking
- Automated EMU/TAR/TUR
- Interval Analysis
- Standards Failure Analysis
- Conformance Testing
- Guard Banding
- Reverse Traceability to Test Point Level

REPORTING TOOLS
- Integrated Custom Reports
- Report Management System
- Multiple Alternate User Reports
- Turn-around Time Reports
- Margin Reports

MANAGEMENT TOOLS
- Production Tracking
  - ◊ Status and Scheduling
  - ◊ Workload Planning/Management
  - ◊ Vendor Tracking
  - ◊ Intralab Communications
  - ◊ Customer Status Reports
- Calibration Asset Management
- Process Control
- Standards Utilization Tracking

ADMINISTRATION TOOLS
- Robust Security and Audit Trail
- Documents/Reports
- Shipping and Invoicing Functions
- Revision Control
- Calibration Cost Tracking
- Paperless Calibration History
- Remote Operation

GENERAL FEATURES
- U.S. Patent #7406388
- Barcode Compatible
- E-Sign Password Transaction Protection
- Integrated Email Profiles

Call Us Today: 800-266-2299
Or Visit Online: edisonmudcats.com

EDISON ESI
A SOUTHERN CALIFORNIA EDISON℠ Company

Transcat Completes Acquisition of Anacor Compliance Services, Inc.

ROCHESTER, NY, July 16, 2012 - Transcat, Inc. (Nasdaq: TRNS) ("Transcat" or the "Company"), a leading distributor of professional grade handheld test and measurement instruments and accredited provider of calibration, repair and other measurement services, announced today that it has acquired Anacor Compliance Services, Inc. ("Anacor"), a nationally recognized and respected provider of specialized analytical, calibration, compliance and validation services to the life sciences sector including the biotechnology, medical device, and pharmaceutical industries.

Headquartered in Furlong, Pennsylvania, Anacor specializes in process validation and compliance qualification with protocol development and execution, as well as final qualification documents. In addition, Anacor provides software and network validation, air sampler, particle counter and pipette calibration along with GC, HPLC and UPLC qualification services and temperature mapping validation services.

Anacor has achieved ISO9001:2008 certification in five essential compliance service components for businesses operating within the Life Sciences Service Sector. Anacor's certification scope includes Calibration Services, Analytical Instrument Qualification Services, Equipment and Process Validation Services, Calibration Laboratory Services, and Customer Asset Management Services.

With over 40 years combined experience, Anacor was founded in 2008 by Reese Barnum and Michael Branvold, who have joined Transcat together with Anacor's 23 employees.

Charles P. Hadeed, President and CEO of Transcat, commented, "Consistent with our growth strategy, this acquisition provides for an expanded suite of quality based services to our targeted life sciences industry customer base. We believe this addition capitalizes on the strength of our infrastructure and reputation for quality, service and integrity."

The terms of the transaction were not disclosed.

More information about Transcat can be found on its website at: transcat.com.

Alcohol Breath Analyzers Can Be Calibrated By Means of a New Generator

A generator has been developed at PTB which produces water-saturated gas mixtures with a defined ethanol content and, for the first time, produces these gas mixtures in a dynamic gravimetric way. Apart from enhancing the basis of the calibration of alcohol breath analyzers, it will improve the traceability of ethanol concentration to the SI units.

Since 1998, evidential breath analyzers have been permitted for use in alcohol tests carried out by the police in road traffic. In Germany, they are an essential part of legal metrology and require a type approval from PTB before being used. For these tests, calibration gas mixtures are produced in PTB, which simulate the breath of a person who is under the influence of alcohol. The gas mixtures consist of air, water and ethanol in a precisely known composition and – to date – had been produced by the usual international saturation method. Here, an air stream is passed through an ethanol-water solution and enriched with ethanol and water until it is saturated. The concentration of ethanol in the gas stream is calculated via distribution coefficients which were determined empirically. In the literature, however, various values are to be found for them.

With the new generator developed at PTB, the gas mixtures can be produced in a dynamic-gravimetric way. The core of the generator is a weighing system with which the mass flows of ethanol and water are determined by the quasicontinuous weighing of the storage containers. The air is dosed via thermal mass flow controllers. The liquid components ethanol and water are injected into the carrier gas flow made of synthetic air and vaporize there completely. As the mass flows of the components are determined individually before mixing, the composition of the gas mixture can be traced directly back to the SI base unit of mass, the kilogram. The use of empirical values from the literature is, thus, no long necessary.

The measurement uncertainty of the ethanol concentration in the gas mixture of the new generator was clearly reduced in comparison to the saturation method.

In the future, the generator can also be used to produce gas mixtures with other components e.g. acetone or carbon dioxide, to calibrate other types of sensors.

Source: http://www.ptb.de/en/publikationen/news/html/news102/artikel/10202.html.

Agilent Technologies 1000B Series Oscilloscopes for Limited Budgets

Agilent Technologies Inc. introduced the 1000B Series oscilloscopes. The four new two-channel models, with bandwidths from 50 MHz to 150 MHz, offer powerful capabilities at an attractive price for engineers, technicians and educators.

The 1000B Series oscilloscopes offer features not normally found on oscilloscopes in this class:

Powerful signal capture and display: All models in the 1000B Series are equipped with a sharp color LCD display that is easy to read even from wide angles. With up to 16 kpts of memory per channel, the 1000B Series provides up to six times more memory than other scopes in its class. In addition, its 1-GS/s sample rate provides excellent signal detail.

Advanced measurement capability: All 1000B Series oscilloscopes can display 23 automatic measurements, including those made with a built-in frequency counter. The 1000B Series comes standard with go/no-go mask testing capability, which allows even inexperienced oscilloscope users to perform precise parametric tests. These scopes also offer advanced capabilities like sequence mode. Sequence mode allows users to record and replay up to 1,000 occurrences of a trigger for easy identification of glitches and other anomalies.

Accelerated productivity: The user interface and front-panel labels on the 1000B Series are available in 11 languages to support worldwide teams. USB connections make it easy to share and document measurement results. A free educator kit helps teachers and professors teach essential oscilloscope skills.

The 1000B Series is ideal for educational institutions that have tight budgets but want to teach their students on real-world equipment. Engineers, technicians and hobbyists with limited budgets also will be able to take advantage of the value offered by the1000B Series.

Additional information about Agilent's new 1000B Series oscilloscopes is available at www.agilent.com/find/1000BSeries.

Agilent's complete portfolio of oscilloscopes is available in a variety of form factors, from 20 MHz to 90 GHz, offering industry-leading specifications and powerful applications.

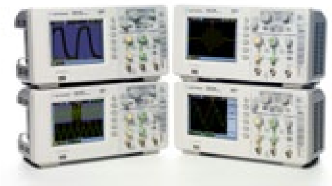

Cal Lab Solutions Releases Free Automated Procedures for the Agilent DSO-X

Cal Lab Solutions Inc. recently released automated procedures for the Agilent DSO-X 20xxA/30xxA and MSO-X 20xxA/30xxA Series oscilloscopes. This procedure was developed for Agilent Technologies, to be licensed to all Agilent customers absolutely free. This procedure comes with three standards configurations: Fluke 5520A with scope option, 5820A, and the 9500A/B with 4 heads.

For a complete list of supported models, visit http://www.callabsolutions.com/products/.

Fluke 52120A Transconductance Amplifier

Fluke® Calibration introduces the 52120A Transconductance Amplifier, which expands calibration capabilities to a broad array of power and energy meters, clamp meters, current transformers and Rogowski coils (e.g. Fluke i6000 iFlex) up to 6000 A. Its industry-leading amplifier accuracy ensures precise calibration of devices.

The 52120A Transconductance Amplifier:

- Supplies dc current to 100 A and ac current up to 120 A at accuracies to 140 ppm
- Generates 3000 or 6000 A when using accessory coils
- Can output up to 360 A when three amplifiers are connected in parallel
- Has inductive drive capability of 1 mH and compliance voltage of 4.5 V

The 52120A is designed for users whose ability to address their high-current calibration workload is limited by the output current, accuracy and drive capacity of their current test equipment. This includes calibration professionals in a calibration/standards lab or electrical utility, manufacturers of power/energy instrumentation and meters, as well as users of electrical test and measurement equipment.

The amplifier operates with any calibrator, signal generator or power supply capable of sourcing 2 V or 200 mA dc or ac, including the Fluke 5080A, 5500 and 5520 Series Multi-Product Calibrators, 5700 Series Multifunction Calibrators, and the 9100 Universal Calibration System. It can also operate in closed-loop mode, seamlessly communicating with Fluke Calibration 610X Electrical Power Standard to deliver enhanced 52120A accuracy.

The Fluke Calibration 52120A Transconductance Amplifier is available now. For more information, visit www.flukecal.com/52120A.

Yokogawa EY200 Digital Earth Tester

Yokogawa Corporation of America is pleased to announce the release of another high quality and well-engineered product, the EY200 Digital Earth Tester. The EY200 will measure earth resistance up to 2,000 ohms using the two pole or three pole methods. It is extremely simple to use via one button and one switch operation. The EY200 is compact, lightweight and includes a complete test kit.

The Yokogawa EY200 was developed for maintenance personnel and technicians to help insure proper wiring and grounding of electrical equipment and systems. Confirming the proper wiring and grounding will help to reduce power quality issues and potential safety hazards. The Yokogawa EY200 compliments the Yokogawa portfolio of portable test instruments, including digital multimeters, clamp-on meters, insulation testers, and portable power monitors.

The Yokogawa EY200 is dust and water resistant (IP54 rated), CE compliant and CAT III 300 V rated. Standard accessories provided with the unit are two and three pole test leads, earth spikes, soft case, shoulder strap, 6 AA batteries and an instruction manual.

The Yokogawa EY200 is available through Yokogawa distributors and representatives at a suggested list price of $575. For more information on the Yokogawa EY200 Digital Earth Tester and additional Yokogawa Meter and Instruments products, visit www.yokogawa-usa.com or contact us via email at meters-instr@us.yokogawa.com.

AKTAKOM'S Power Supply with Remote Control

T&M Atlantic., distributer of the test and measurement equipment, unveiled Aktakom APS -7303L and APS-7305L Power Supplies. These models are the most economical, programmable, regulated, remote controlled power supplies on the market. Precision and stability of APS-73xxL series exceeds the norms of similar equipment. The major advantage of 73xxL series power supplies is the ability to be remote controlled via LAN or USB. Innovative software called AKTAKOM POWER MANAGER allows user to set and pre-set inputs, graph, as well as, time control the power supplies output. AKTAKOM POWER MANAGER works on any PC, IPHONE, IPAD or Android mobile device. MADE IN USA. More info available at www.tmatlantic.com.

Mountz LPX Torque Sensor

Mountz, Inc., a specialist in the design and manufacture of torque control products, offers the new LPX torque sensor for testing small torque tools. The LPX is a low torque sensor designed for calibrating and testing small hand screwdrivers, torque wrenches and power tools. With its low profile design, the calibration instrument can be used for automated applications, by mounting it to a palletized system. This saves time as there is no need to remove the robotic electric screwdriver from the robot or off the automated system for calibration. These versatile torque sensors are used in conjunction with a torque tester. Mountz offers various models covering a torque range from 1 inch-ounce up to 20 inch-pounds.

Small torque tools go out of calibration with use. To maintain consistent accuracy, small torque tools must be checked periodically for wear or defective parts.

A small power or hand torque tool is a measuring tool that must be properly calibrated and maintained. Torque testing also ensures torque equipment is operating to peak performance and can highlight potential tooling problems before they arise perhaps due to tool wear or broken components. Only Mountz LPX torque sensors provide precision torque testing for these applications.

In the manufacturing and assembly world, tightening, controlling, or measuring torque fasteners is imperative for production efficiency.

Using a quality torque sensor, like the LPX, and a torque tester has become increasingly important for many companies to ensure that proper torque control is being applied and monitored. Testing torque is a science and not something that can be left to chance.

For more information, visit : www.mountztorque.com.

Hybrid Instruments' Mixed Field Analyzer

A new mixed field analyzer (MFA) has been invented that eliminates post processing. The instrument provides real time event processing for fast organic liquid scintillation detectors.

Hybrid Instruments, with BNC Scientific,unveiled the newest Mixed Field Analyzer at SORMA West May 14-17, 2012 in Oakland, California. Prof. Malcolm Joyce and Dr. Frank Cave, Co-Founders of Hybrid Instruments, have invented a self-contained real-time digital Pulse Shape Discrimination (PSD) system. This versatile MFAcan be used with a range of fast scintillation detectorsfor real-time PSD and timing applications, and comes with a dedicated analysis package.

Hybrid Instruments' Mixed Field Analyzer splits gamma rays and neutrons, particularly fast neutrons, on the fly. The Mixed Field Analyzer's outputs are synchronized with the time of arrival of the event, allowing for coincidence measurements to be made. This synchronization eliminates the need to repeat the experiment/event. This is particularly important if the environment being measured is difficult to access or repeat.

"If you are working in an environment that perhaps is difficult to get access- if you have to post process- then you're never quite sure if you have enough data." said Prof. Malcolm Joyce, Co-Founder of Hybrid Instruments and co-inventor of the Mixed Field Analyzer. "So, with this [Mixed Field Analyzer} because its real time, you run it for as long as you want to until you've collected a sufficient amount as opposed to coming out of the environment, post processing, and saying 'ok, we need to go back in'. For organic scintillators the MFA is all you need: strap two MFAs together and you've got the basis for neutron coincidence measurements."

Hybrid Instruments' Mixed Field Analyzer is the latest technology in gamma neutron separation. SORMA West was the United States premier, with BNC Scientific as the proud sponsor.

About the Company: BNC Scientific, a division of Berkeley Nucleonics Corporation, is available to address growing demands in the scientific community with strong, US-based service and application support. We offer a high degree of attention to each application with unparalleled use of technology resources. BNC Scientific represents best-in-class instrumentation for applications in research.

For more information on Mixed Field Analyzers or other Nuclear and Radiation Spectroscopy, call 866.276.6188 or email info@bncscientific.com

Additel ADT761 Automated Pressure Calibrator

Additel Corporation is excited to introduced the new ADT761 Automated Pressure Calibrators. With a built-in high performance electronic pump and precision pressure controller, the ADT761 series automated pressure calibrators provide a turn-key solution for calibration of gauges, transmitters, and switches both in the field and in the laboratory.

In a portable package, this innovative calibrator can automatically generate from 90% vacuum to 375 psi (25 bar) pressure with 0.005%FS pressure control stability and 0.02%FS accuracy. To improve the calibrator accuracy, two pressure modules with differing ranges are used. These are built-in and integrated with the internal pump and controller. With optional external pressure modules (ADT160 series), the ADT761 can measure pressures up to 10,000 psi (700 bar) with 0.025%FS accuracy. In addition to the pressure generation, control, and measurement capabilities, the ADT761 also features HART communication capability, supplies 24V loop power, and reads the current or voltage produced by the pressure transducers.

A built-in contamination prevention system can prevent contamination of the calibrator from dirty devices under test. The contamination prevention system is composed of a filter, a liquid trap and a venting system. The solid particles are blocked by the filter, a small amount of liquid can be collected by the liquid trap. Both solid particles and liquid can be blown out through venting system automatically. The state of art ADT761 automated pressure calibrator brings automated pressure calibration to the field.

For more information, please visit www.additel.com.

Calibrating DC Shunts: Techniques and Uncertainties

Jay Klevens
Ohm-Labs, Inc.

Accurate electrical current measurement is critical to the power and electrical test industries. DC and low frequency AC current is usually measured using a current shunt. Shunt calibration has unique error sources which must be properly applied to obtain valid measurements.

I. Introduction

DC and low frequency AC current is usually measured with a shunt, using Ohm's law: I=E/R. If resistance (R) and voltage (E) are known, current (I) can be calculated. A multimeter has an internal shunt and measures voltage across it to calculate and display current. Higher current measurements use external shunts.

Shunts are resistors, subject to similar measurement methods, uncertainty budgets and calibration controls. However, unlike most resistance standards, shunts are subjected to higher current, and thus higher power. Power (in watts) is calculated by $W=I^2R$. A typical resistance standard is designed for 10 mW power, whereas shunts can exceed 100 W.

The challenge in calibrating shunts is to perform accurate resistance measurements at high power levels [1].

Two types of shunts are in wide use: metrology type shunts designed for calibration use and lower cost metering type shunts. Error sources for both are the same, although generally lower for metrology type shunts.

Original Equipment Manufacturer (OEM) manuals for shunts often make no mention of common error sources which can contribute significantly to measurement uncertainty.

To estimate measurement uncertainty, it is important to evaluate both 'Built-in' (type B) uncertainty components of the measurement system and 'At-the-time-of-test' (type A) contributions of the unit under test.

II. Calibration Methods

Shunts are measured by comparison, either with a resistance standard using a current comparator bridge, or with a calibrated standard shunt [2].

For the bridge comparison method a bridge with a range extender allows direct comparison of high current through a shunt with lower current through a calibrated resistance standard. The advantage of this system is its theoretical measurement uncertainty of a few µΩ/Ω (ppm) at high current. The disadvantage of this method is its high cost.

The shunt comparison method compares the voltages across two shunts in series. It requires only a power source, a standard shunt and two voltmeters. However, the accuracy is lower than a bridge system.

Both methods are equally subject to most type A uncertainty contributions of the shunt under test.

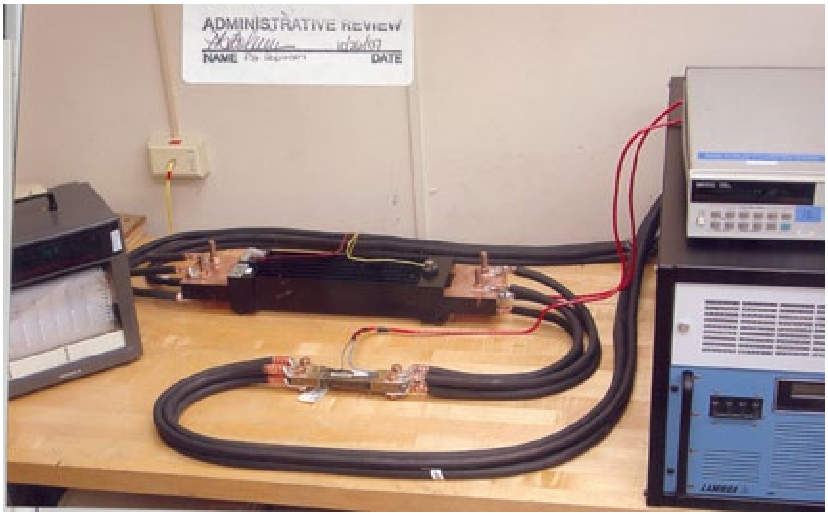

Figure 1. Shunt comparison system (courtesy BWX Technologies).

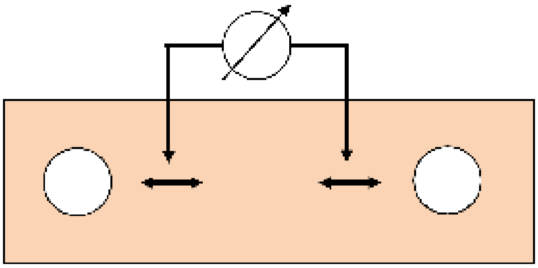

Figure 2. Four-wire connection errors.

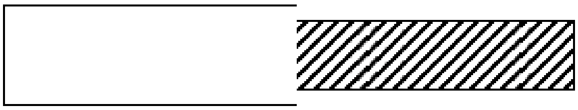

Figure 3. L&N shunt current connection bar.

III. Error Sources

Error sources in calibrating shunts are:

1. Connection
2. Temperature
3. Frequency
4. Drift
5. Thermal EMF

Connection errors are due to shunts being four-wire resistors. Current flows through the resistor via current connection points; voltage is measured across potential points. As shown in Figure 2, moving the potential points towards the center of the shunt lowers the measured resistance; moving them towards the ends increases the measured resistance.

On metering shunts with screw connections to a brass block, connecting under the outside of the screws will give a higher resistance than inside of the screws. The difference between two measurements at these two points will give an estimate of the type A potential connection error.

Most metrology type shunts have a wire or post leading away from the the shunt, which minimizes potential connection errors.

Similarly, changing the position of current connections changes the relative position of the potential points, which changes measured resistance. Changing current connections from one side of a block to the other changes the resistance. On shunts with more than one bolt hole, changing from one hole to another will change resistance [3].

Current connection blocks are not perfect conductors. Current distribution through a shunt changes with surface cleanliness and both torque and material of the connecting bolts. It is helpful to clean the current connection surface with an abrasive pad and to use silicone bronze hardware of a diameter to match the holes. Bolts should be firmly torqued (20-30 nm).

If both sides of a current block are accessible, connect to both sides. If there are two holes, connect to both sides of both holes.

If your standards include metering type shunts, connection errors can be reduced by permanently affixing potential and current lead wires and specifying calibration with these cables.

On Leeds & Northrup type shunts, current connection should never be made to the tops of the posts, but through the holes in the current posts. Variations can be reduced by permanently installing a bar with the same diameter as the hole, with one end threaded for lug connections, as shown in Figure 3. To avoid the surface resistance of oxidized copper, use plated copper or 385 alloy brass.

Performing several measurements with different current connections can give an estimate of type A current connection errors.

In metering type shunts, potential and current connection errors can exceed 0.1%.

Temperature errors are caused by heating of a shunt under power and by ambient temperature variations.

All metals change resistance with temperature. Many shunts use a copper-manganese alloy called Manganin, which typically has a temperature coefficient of resistance (TCR) of about 20 μΩ/Ω/°C. A 50 °C rise in temperature under power can cause a 1000 μΩ/Ω (0.1%) change in resistance.

TCR is not linear. Measurement at low current will not predict the resistance at higher currents. Failing to calibrate a shunt through its full useable current range is failing to calibrate it.

Note that most metering shunts are designed for a maximum of 2/3 rated current (1/2 is a safer limit). Metering shunts taken to full rated current will likely be permanently damaged, while most metrology shunts are designed to handle full rated current.

A shunt continues to change resistance until it reaches thermal equilibrium at the applied current. For large, high current shunts, this can take over an hour. Only at this point should measurements begin [2].

Heat distribution in a shunt also affects its resistance. Smaller gage cables and lugs can add heat to the shunt. Larger gage cables and lugs can act as heat sinks, lowering the temperature of the shunt. Thermal uniformity errors are difficult to evaluate without thermal imaging

General Guidelines

1. **Clean current & potential connection points**
2. **Connect potential with a single loop of solid bare copper wire**
3. **Connect current with silicon bronze bolts of proper diameter**
4. **Torque securely**
5. **Connect current lugs in line with shunt**
6. **Use both sides of all holes**
7. **Size cables & lugs or bus to introduce minimal heat**
8. **Allow full thermal stabilization at each applied current**
9. **Calibrate through full rated current**
10. **Disconnect & repeat on separate days for repeatability**

equipment or a series of temperature sensors along the shunt element. These errors are also impractical to duplicate from one lab to another.

Heat transfer from a shunt at thermal equilibrium is also affected by ambient temperature and air flow velocity; this affects the resistance value from lab to lab.

Bonding a temperature sensor to the center of the shunt element and performing a current/temperature characterization can generate a table of corrections which can be applied at a given temperature, reducing temperature uncertainty.

Frequency errors are caused by inductive components of the shunt (generally small) and by AC coupling to the voltage measurement lead wires. At line frequency (50/60 Hz), coupling errors can be minimized by arranging current cables in line with the shunt, and by arranging potential wires into a twisted pair extending at right angles from the shunt (as shown in Figure 1).

The AC/DC difference of most shunts at line frequency is generally below the uncertainty of AC/DC difference measuring systems, so the DC resistance may be used with reasonable assurance.

Higher frequency current measurement requires specially designed AC shunts.

Drift errors depend on the long term stability of the shunt. Shifts can be caused by handling, shipping, or application of excess current. Because of the often elevated temperature of shunts, drift over time can be accelerated. Periodic recalibration can establish long term drift.

Measuring a shunt before and after recalibration can reveal shifts caused by physical damage. Shock or excessive torque can crack the solder joints between current blocks and shunt blades, increasing the resistance.

Thermal EMF errors are caused by a thermocouple effect at the potential junctions of shunts. At higher temperatures, this effect becomes stronger. Thermal EMF errors may be canceled by reversing the current flow and averaging the forward and reverse measurements. Bridge systems have a reversing switch to cancel thermal EMF errors.

IV. Shunt Calibration Uncertainty Budgets

Uncertainty budgets for shunt calibration is the root sum square (or more conservatively the addition) of type B system components and type A components unique to the test.

For current comparator bridge systems, type B components include:

1. The resistance standard (including temperature, drift, etc.)
2. The current comparator bridge
3. The range extender

For a shunt comparison system, type B components include:

1. The standard shunt (including temperature, drift, etc.)
2. The standard voltmeter
3. The unit under test voltmeter

Type A uncertainties are variable and largely dependent on the type of shunt and the care taken during measurement. A rough estimate of common factors, without extensive characterization, can include:

1. Connection errors
   a. Metering shunt potential connection, 50 µΩ/Ω
   b. Metering shunt current connection, 100 µΩ/Ω
   c. Metrology shunt current connection, 50 µΩ/Ω
   d. Standard deviation of separate tests with differing connections
2. Temperature errors, after stabilization at applied current
   a. Manganin shunt, +/-20 µΩ/Ω/°C ambient temperature uncertainty
   b. Standard deviation of separate tests on separate days
3. Drift error
   a. Standard deviation of separate tests on separate days
   b. Pre and post recalibration tests

4. Frequency error
   a. For 50/60 Hz, 50 μΩ/Ω with proper lead wire placement
5. Thermal EMF error
   a. Canceled by averaging forward and reverse current measurements

V. Conclusion

Connection, temperature, frequency, drift and thermal emf errors in shunts are common, particularly in older lab and metering type shunts. Understanding and accounting for these errors can improve the accuracy of shunt measurement and can assist in developing realistic uncertainty budgets.

References

[1] D. W. Braudaway, "Behavoir of Resistors and Shunts: With Today's High-Precision Measurement Capability and a Century of Materials Experience, What Can Go Wrong?," *IEEE T. Instrum. Meas.*, vol. 48, no. 5, pp. 889-893, October 1999.

[2] R. E. Elmquist, D. G. Jarrett, G. R. Jones, M. E. Kraft, S. H. Shields, and R. F. Dziuba, "NIST Measurement Service for DC Standard Resistors," *NIST Technical Note 1458*, December 2003.

[3] M. Kraft, "Measurement Techniques of Low-Value High-Current Single-Range Current Shunts from 15 Amps to 3000 Amps" *Measure Magazine*, V. 2, No. 1, March 2007.

Jay Klevens, Ohm-Labs, Inc., 611 E. Carson St., Pittsburgh, PA 15203, (412) 431-0640, jklevens@ohm-labs.com.

Quality of Air Speed Calibrations

Rachael V. Coquilla
Bryza Wind Lab

Wind measuring instruments, such as cup anemometers, propeller anemometers, ultrasonic anemometers, velocity meters, airflow meters, and many other types, are commonly used in various industries as monitoring devices or for evaluation and research of air movement. The most common application is weather measurements. In some cases, high accuracy in measuring atmospheric winds is not necessary. Thus, a simple field check, where the output of a wind sensor is verified against a known reference installed nearby, may be all that is required. However, for industries where wind speed measurements are critical such as wind energy, nuclear safety, and building commissioning, wind measuring instruments are required to be calibrated in a controlled wind tunnel test facility, where the reference wind speed measurement is traceable to national standards. There are several types of wind tunnels, each of which were designed for specific purposes. As specified by various published standards, wind instrument calibration testing is to be performed in a uniform-flow, low-turbulence wind tunnel. Such standards define the minimum requirements to meet and maintain steady-state horizontal flow in an empty wind tunnel test section. However, once a test object is placed in that steady flow, the flow quality changes. It is then recommended to evaluate the flow quality due to the disturbance caused by the test object and resulting interaction from the wind tunnel test section boundaries. The combined effect of test object disturbance and wall interaction is commonly known as "blockage" and is one of the most challenging phenomena associated with wind tunnel studies. If the level of "blockage" during a wind sensor calibration test affects the relationship between the output of the instrument under test and the corresponding reference wind, the test design may need to be adjusted and/or correction factors may need to be applied to the corresponding test results. The purpose of this paper is to discuss the investigative methods when qualifying a wind tunnel for air speed calibration of wind measuring instruments and present the evaluation results of a newly installed wind tunnel for air speed calibration testing. Overall, the qualification of a wind tunnel to conduct air speed calibrations not only depends on how well the facility satisfies the minimum requirements from published standards but also is related to how a specific wind measuring instrument performs in that wind tunnel.

Introduction

Several methods have been used to calibrate wind sensors including comparisons to a reference sensor on a meteorological tower or even on a moving vehicle. Since most end-user applications typically expose wind instruments to turbulent flows, particularly those that are used for weather measurements, it would seem that a calibration should also be performed in the same conditions. However, such unsteady surroundings generally introduce additional factors that greatly increase uncertainty in the measurements, both in the reference and the test instrument readings. In order to maintain better control, test standards specify that air speed calibration of wind measuring instruments is to be performed in a wind tunnel facility that is capable of maintaining uniform, steady wind speeds at low turbulence. Such a facility assures that the raw output of a wind sensor is related, hence calibrated, to only the horizontal component of the incoming wind. The response of a wind sensor due to other conditions such as flow angularity are then evaluated through further controlled sensitivity tests.

Test Facility Requirements

Generating the desired steady-state conditions in a wind tunnel is considerably trivial, but is also challenging to achieve. There are various wind tunnels that are used for specific types of testing. For anemometer calibration, test standards have specified certain parameters to be maintained in order to have uniform, low-turbulence flow in the wind tunnel test section. The following table (Table 1) displays a summary of minimum wind tunnel requirements defined by test standards commonly referred for the calibration of meteorological wind sensors.

From the list of wind tunnel characteristics in Table 1, base performance of a wind tunnel is defined by the wind speed capability, flow uniformity, horizontal wind gradient, turbulence intensity, air density uniformity, and data acquisition resolution. Such characteristics are surveyed with no test instrument installed in the test section. To fully qualify a wind tunnel to perform wind sensor calibration testing, it is also critical to evaluate the effect of blockage in the wind tunnel test section due to the presence of a test object. Generally, once an object

Wind Tunnel Characteristic	Description	Summary of Minimum Requirements from Standards
Wind Speed Capability	Controlled wind speed range	IEC 61400-12-1: generate controlled speeds from 4 to 16 m/s ASTM D 5096-02, ISO 17713-1: produce speeds at least from 0 to 50% of application speed and maintained within +/- 0.2 m/s ASTM D 6011-96: generate speeds of at least 1 to 10 m/s within +/- 0.1 m/s or better ISO 16622: produce speeds over full application speed and maintained within +/- 0.2 m/s, preferably +/- 0.1 m/s
Flow Uniformity	Percent difference in wind speed or velocity profile within the test section volume	IEC 61400-12-1: less than 0.2% ASTM D 5096-02, ASTM 6011-96, ISO 17713-1, and ISO 16622: uniform velocity profile to within 1%
Horizontal Wind Gradient	Pressure differential at the area covered by a rotating sensor	IEC 61400-12-1: must be less than 0.2%
Turbulence Intensity	Ratio between the wind speed standard deviation to its mean	IEC 61400-12-1: must be less than 2% ASTM D 5096-02, ASTM 6011-96, ISO 17713-1, and ISO 16622: must be less than 1%
Air Density Uniformity	Percent difference in density within test section volume	ASTM D 5096-02 & ISO 17713-1: less than 3% difference
Data Acquisition Resolution	Method of collecting reference wind speed data	IEC 61400-12-1: maintain resolution of 0.02 m/s, sample frequency of at least 1 Hz for 30 sec ASTM D 5096-02, ASTM 6011-96, ISO 17713-1, and ISO 16622: maintain resolution of 0.02 m/s, sample frequency of at least 10 Hz for 30 to 100 sec
Blockage	Ratio of the wind sensor projected area plus mount to the test section cross-sectional area	IEC 61400-12-1: not to exceed 10% for open test sections and 5% for closed test sections ASTM D 5096-02, ASTM 6011-96, ISO 17713-1, and ISO 16622: less than 5%, preferably closer to 1%
Repeatability	Consistency of repeated tests	IEC 61400-12-1: repeated reference tests are repeatable to less than 0.5% at 10 m/s
Interlaboratory Comparison	Comparison to other test facilities	IEC 61400-12-1: “round robin” testing with other calibration facilities are within 1% over the range of 4 to 16 m/s

Table 1. Minimum Wind Tunnel Requirements.

is inserted into and blocks the wind tunnel test section, the flow around the object increases. This is particularly challenging when the object under test is a mechanical or rotating wind sensor. Such a change in the flow regime requires that correction factors may be required to the calibration of the wind sensor. Another criteria beyond the base wind tunnel performance is the repeatability of tests from reference sensors. Repeatability is evaluated from multiple calibration of an assigned sensor similar to the model that is to be regularly calibrated. According to the test standard, IEC 61400-12-1, the sensor output at the test point of 10 m/s is to be within 0.5% repeatable. A final criteria for the qualification of a wind tunnel to perform wind sensor calibrations is a comparison with other similar test facilities. IEC 61400-12-1 also specifies that the calibration results for the test range of 4 to 16 m/s are to be within 1% in comparison to other wind tunnel laboratories. Thus, in addition to meeting the requirements that define the base performance, the qualification of a wind tunnel to perform wind sensor calibrations also include: 1) an evaluation of the flow interaction between the test sensor and the wind tunnel boundaries, 2) the repeatability of a reference sensor, and 3) the consistency with other similar facilities.

Figure 1. Photos of Aero-Subsonic Wind Tunnel (AWST1) and wind sensor under test (on the right).

Aero-Subsonic Wind Tunnel at Bryza Wind Lab

A new Aero-Subsonic Wind Tunnel (ASWT1) was recently installed at Bryza Wind Lab, located in Fairfield, California. This wind tunnel is an open-circuit, closed test section wind tunnel that has a test section size of 2.5 ft height x 2.4 ft width x 5 ft length (0.754 m x 0.754 m x 1.54 m). With a 50 hp fan-motor that is controlled by a variable frequency drive (VFD), the wind tunnel is capable of test section speeds of up to 47 m/s. One of the main types of tests that will be performed with this wind tunnel is calibration testing of meteorological wind sensors (see Figure 1). Thus, the flow in the test section was designed to maintain uniformity, low turbulence, and steady speeds.

In general, flow characteristics in an open-circuit wind tunnel test section are a result from the shape of the upwind contraction section and are stabilized by the specific diversion angle in the downwind diffuser section. According to Bernoulli's equation and the conservation of mass, the speed in the test section is fundamentally related to the difference in pressure between the inlet and outlet of the contraction section. The symmetric, polynomial shape of the contraction is designed so that boundary layer development is minimized, hence resulting to a uniform test section. To maintain the developed flow inside the test section, a downwind diffuser section is included and designed with a particular diverging angle that minimizes boundary layer separation.

Base performance for the wind tunnel was verified using the recommended procedures in AIAA R-093-2003, "Calibration of Subsonic and Transonic Wind Tunnels." Wind tunnel calibration procedures in AIAA R-093-2003 essentially define the relationship between the dynamic pressure in the test section to the pressure drop across the contraction section. In ASWT1, this relationship is represented by the differential pressure measurement from Pitot-static tubes installed at the inlet of the test section, where the total and reference pressures are ported to an electronic differential pressure transducer. Also measured in the test section are the local conditions of ambient pressure, temperature, and relative humidity. Thus, the velocity, V, from the Pitot-static tube system is calculated as follows:

$$V = \sqrt{\frac{2\Delta p}{\rho}} \ . \qquad (1)$$

Here, Δp is the differential pressure and ρ is the local density, which is calculated with a correction for humidity. The local density is calculated according to the following equation:

$$\rho = \frac{1}{R^{*}T}\left[PM_{air} - 2.05\times10^{-7}\phi e^{0.0631846T}\left(M_{air} - M_{w}\right)\right] , \qquad (2)$$

where T is the test section temperature, P is the ambient pressure, ϕ is the relative humidity, R^{*} is the universal gas constant, M_{air} is the molar mass of air, and M_{w} is the molar mass of water. With Equations 1 and 2, the control voltage to the fan-motor VFD was calibrated to the velocity obtained from the Pitot-static tube system (see the following Figure 2). This calibration also showed that the voltage input to the fan-motor VFD is linearly related to the test section speed.

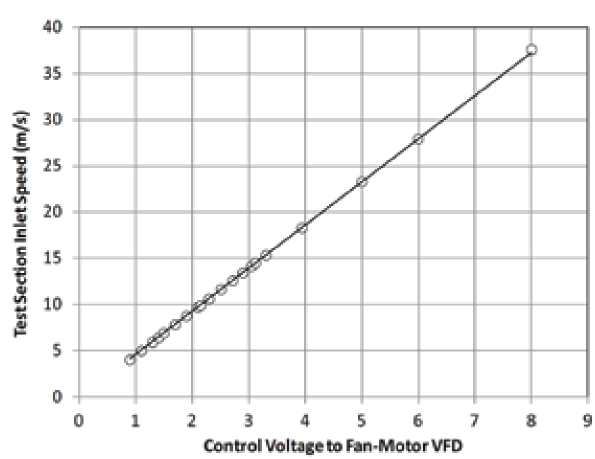

Figure 2. Calibration plot of wind tunnel fan-motor VFD to test section inlet speed.

To verify the test section uniformity, cross-section profiles at four wind speed settings were obtained at the center of the test section. These profiles were measured by positioning a Pitot-static tube at equally distributed points along the center downwind plane of the test section. The following Figures 3 to 6 display the actual and relative velocity profiles in the wind tunnel test section of AWST1. Relative velocity profiles were generated by normalizing the local traverse wind speed measurement to the average wind speed near the center of the test section. Overall, flow conditions in the test section are maintained to within 0.01% uniformity.

From the velocity profile surveys, a preliminary indication of the test section turbulence was determined to be less than 0.1%. This was only estimated from the average steady-state variability of the speed measurements sensed from the inlet Pitot-static tubes. For wind sensor calibration testing, this estimation of turbulence is acceptable; however, further evaluation using measuring systems with higher sensitivity and resolution, such as hot wire anemometry, is required. Comparing the wind speeds measured from the velocity profiles at the center of the test section to the wind speeds measured from the Pitot-static tubes at the test section inlet, there was an average deviation of +0.014%. Although this deviation is relatively small, it is used as a correction to the measurements at the inlet. Since test models come in various shapes and sizes, the appropriate position correction to the inlet Pitot-static tubes will also depend on the critical location at which the model senses the flow.

Test Qualification of a Model C3 Wind Sensor

A wind sensor model that is planned to be regularly tested in ASWT1 is a Second Wind Model C3 anemometer. This wind sensor is a rotating cup anemometer that produces a sine wave output signal generated by the interaction between a rotating magnet and a stationary coil. The output of the

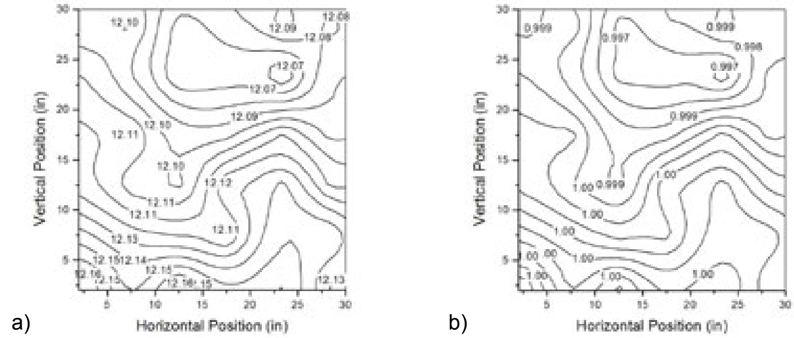

Figure 3. a) Velocity profile at average 12.1 m/s, b) Relative velocity profile at average 12.1 m/s.

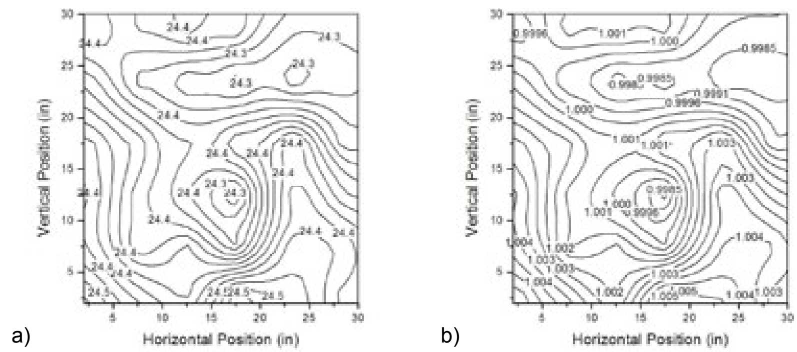

Figure 4. a) Velocity profile at average 24.5 m/s, b) Relative velocity profile at average 24.5 m/s.

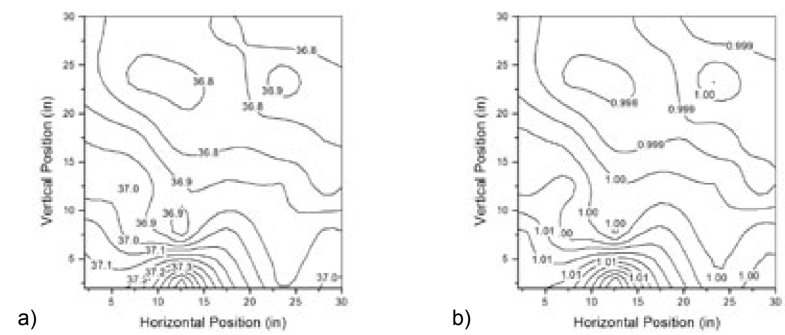

Figure 5. a) Velocity profile at average 36.9 m/s, b) Relative velocity profile at average 36.9 m/s.

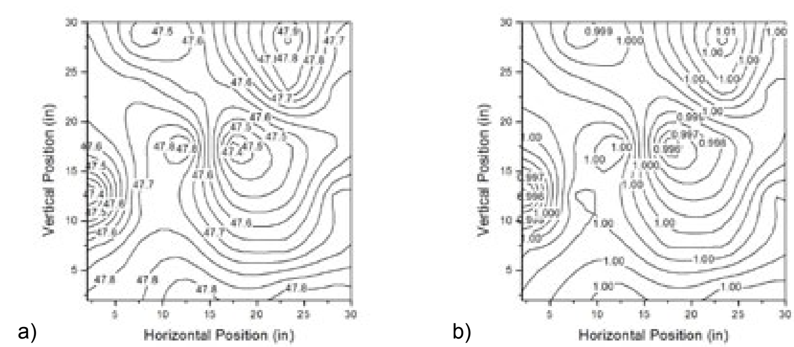

Figure 6. a) Velocity profile at average 47.7 m/s, b) Relative velocity profile at average 47.7 m/s.

sensor is essentially represented by the frequency of the resulting sine wave, which is calibrated to the reference wind tunnel speed.

This particular model is installed on a 1/2 inch diameter mount with the lower portion of the sensor body covered by a rubber boot. The effective projected area of the wind sensor installation, including the mount and the boot, corresponds to a blockage ratio slightly less than 2%. The recommended blockage correction factor for a closed test section wind tunnel is 0.25 times the blockage ratio. Since ideally the flow increases with a test object installed, the blockage correction multiplied to the reference wind speed measurement at the inlet Pitot-static tubes is 1.005 for a Model C3 anemometer.

Calibrations for a Model C3 anemometer were conducted for a the wind speed range of 4 to 16 m/s. From a set of five repeated tests, a comparison of the resulting sensor wind speeds at 10 m/s was maintained to within 0.2%. Ten additional Model C3 anemometers were also calibrated and compared with the corresponding similarly-performed calibrations from another test facility. Due to confidentiality, actual results from this comparison will not be presented in this paper. However, on average, the variation in the calibration was within 1% between the two test facilities. To further validate the closeness of these two test facilities, future work is needed for additional comparisons with other test facilities.

Uncertainty in the Calibration Test

For a wind sensor calibration, the overall uncertainty is determined from the combined uncertainty contributions from the reference wind speed measurement, the measurement of the output of the wind sensor under test, and the degree of linearity. For the Pitot-static tube system in ASWT1, a velocity equation was defined in Equation 1. However, with the necessary corrections applied, the velocity equation is then modified as follows:

$$V = C_h k_b k_c \sqrt{\frac{2\Delta p}{\rho}} \quad . \tag{3}$$

Here, C_h is the Pitot-static tube head coefficient, k_b is the blockage correction, and k_c is the reference position correction. Combined with the density equation, the expanded velocity equation becomes:

$$V = C_h k_b k_c \sqrt{\frac{2\Delta p R^* T}{PM_{air} - 2.05\times10^{-7}\phi e^{0.0631846\,T}\left(M_{air} - M_w\right)}} \quad . \tag{4}$$

Out of the variables in Equation 4, M_{air} and M_w are deemed independent since the corresponding standard uncertainties are small enough to be considered negligible. The standard uncertainty in R^* is also relatively small and may also be negligible. Thus, independent variables are not included in the uncertainty analysis of the wind

Dependent Variable	Sensitivity Coefficient Equation	Equation Number
Pitot-static Tube Head Coefficient	$\frac{\partial V}{\partial C_h} = k_b k_c \sqrt{\frac{2\Delta p R^* T}{PM_{air} - 2.05\times10^{-7}\phi e^{0.0631846\,T}\left(M_{air} - M_w\right)}} = \frac{V}{C_h}$	(5)
Blockage Correction	$\frac{\partial V}{\partial k_b} = C_h k_c \sqrt{\frac{2\Delta p R^* T}{PM_{air} - 2.05\times10^{-7}\phi e^{0.0631846\,T}\left(M_{air} - M_w\right)}} = \frac{V}{k_b}$	(6)
Position Correction	$\frac{\partial V}{\partial k_c} = C_h k_b \sqrt{\frac{2\Delta p R^* T}{PM_{air} - 2.05\times10^{-7}\phi e^{0.0631846\,T}\left(M_{air} - M_w\right)}} = \frac{V}{k_c}$	(7)
Universal Gas Constant	$\frac{\partial V}{\partial R^*} = \frac{1}{2} C_h k_b k_c \sqrt{\frac{2\Delta p T}{R^*\left[PM_{air} - 2.05\times10^{-7}\phi e^{0.0631846\,T}\left(M_{air} - M_w\right)\right]}} = \frac{1}{2}\frac{V}{R^*}$	(8)
Ambient Pressure	$\frac{\partial V}{\partial P} = -\frac{1}{2}\frac{M_{air} C_h k_b k_c}{\left[PM_{air} - 2.05\times10^{-7}\phi e^{0.0631846\,T}\left(M_{air} - M_w\right)\right]^{3/2}}\sqrt{2\Delta p R^* T} = -\frac{1}{2}\frac{M_{air} V}{PM_{air} - 2.05\times10^{-7}\phi e^{0.0631846\,T}\left(M_{air} - M_w\right)}$	(9)

Dependent Variable	Sensitivity Coefficient Equation	Equation Number
Ambient Temperature	$\frac{\delta V}{\delta T} = C_h k_c k_b \sqrt{2k_c \Delta p R^*} \frac{\begin{array}{c} 0.5(T)^{-1/2}\left[PM_{air} - 2.05\times10^{-7}\phi e^{0.0631846T}(M_{air}-M_w)\right]^{1/2} \\ -0.5\left[PM_{air} - 2.05\times10^{-7}\phi e^{0.0631846T}(M_{air}-M_w)\right]^{-1/2}(T)^{1/2} \\ \left(-0.0631846\left[2.05\times10^{-7}\phi e^{0.0631846T}(M_{air}-M_w)\right]\right)\end{array}}{PM_{air} - 2.05\times10^{-7}\phi e^{0.0631846T}(M_{air}-M_w)} = \frac{1}{2}V\left[\frac{1}{T} + \frac{1.295\times10^{-8}\phi e^{0.0631846T}(M_{air}-M_w)}{PM_{air} - 2.05\times10^{-7}\phi e^{0.0631846T}(M_{air}-M_w)}\right]$	(10)
Relative Humidity	$\frac{\delta V}{\delta \phi} = -\frac{1}{2}\frac{C_h k_b k_c\left[-2.05\times10^{-7}\phi e^{0.0631846\,T}(M_{air}-M_w)\right]}{\left[PM_{air} - 2.05\times10^{-7}\phi e^{0.0631846\,T}(M_{air}-M_w)\right]^{3/2}}\sqrt{2\Delta p R^* T} = \frac{1}{2}\frac{V\left[-2.05\times10^{-7}\phi e^{0.0631846\,T}(M_{air}-M_w)\right]}{PM_{air} - 2.05\times10^{-7}\phi e^{0.0631846\,T}(M_{air}-M_w)}$	(11)
Differential Pressure	$\frac{\delta V}{\delta \Delta p} = \frac{1}{2}C_h k_b k_c \sqrt{\frac{2R^* T}{\Delta p\left[PM_{air} - 2.05\times10^{-7}\phi e^{0.0631846\,T}(M_{air}-M_w)\right]}} = \frac{1}{2}\frac{V}{\Delta p}$	(12)

Table 2. Sensitivity coefficients for dependent variables of reference wind speed calculation.

speed measurement. As an example to verify that such variables would not have an impact in the reference wind speed, an uncertainty analysis is performed for R^*. Thus, the uncertainty in the reference wind speed is a function of the dependent variables, C_h, k_b, k_c, R^*, P, T, ϕ, and Δp. To determine how much each variable is related to the wind speed calculation, the sensitivity coefficients are first derived from Equation 4. Table 2 presents the sensitivity coefficients for each of the dependent variables.

Uncertainty in the reference wind speed measured by a Pitot-static tube system is then defined as:

$$U_V = \sqrt{B_V^2 + (tS_V)^2} \quad . \tag{13}$$

Here, B_V represents the propagation of systematic or bias error contributions (Type B) and is a function of all the dependent variables found in reference wind speed equation. Thus, the propagation of systematic errors is defined as:

$$B_V = \sqrt{\begin{array}{c}\left(\frac{\delta V}{\delta k_b}B_{k_b}\right)^2 + \left(\frac{\delta V}{\delta k_c}B_{k_c}\right)^2 + \left(\frac{\delta V}{\delta C_h}B_{C_h}\right)^2 + \left(\frac{\delta V}{\delta R^*}B_{R^*}\right)^2 \\ + \left(\frac{\delta V}{\delta P}B_P\right)^2 + \left(\frac{\delta V}{\delta T}B_T\right)^2 + \left(\frac{\delta V}{\delta \Delta p}B_{\Delta p}\right)^2 + \left(\frac{\delta V}{\delta \phi}B_\phi\right)^2\end{array}} \quad . \tag{14}$$

For the measured variables, P, T, Δp, and ϕ, bias errors generally originate from data acquisition, signal conditioning, and instrument performance such as linearity or accuracy.

The term S_V in Equation 13 signifies the propagation of random or precision error contributions (Type A) which originate only from the measured dependent variables, P, T, Δp, and ϕ. At 95% confidence, the value of t for infinite (∞) degrees of freedom is 1.96. Hence, the propagation of random errors is defined according to the following equation:

$$S_V = \sqrt{\left(\frac{\delta V}{\delta P}S_P\right)^2 + \left(\frac{\delta V}{\delta T}S_T\right)^2 + \left(\frac{\delta V}{\delta \Delta p}S_{\Delta p}\right)^2 + \left(\frac{\delta V}{\delta \phi}S_\phi\right)^2} \quad , \tag{15}$$

where, S_P, S_T, $S_{\Delta p}$, and S_ϕ, are the standard deviations of the corresponding measured variables.

Figure 7 presents the uncertainty contributions from each dependent variable in the reference wind speed equation. In general, the greatest contribution comes from the correction factors. Of the measured variables, relative humidity, U(RH), gives the smallest effect, while ambient pressure, U(P), and temperature, U(T), are the most noticeable. Errors in the differential pressure also contribute greatly in the lower speeds, which is mainly due to the limited resolution of the transducer. Overall, the reference wind speed uncertainty in ASWT1 ranges from 0.01 to 0.065 m/s for the range of 4 to 16 m/s.

Uncertainty in the output of the wind sensor under test, U_{IUT}, is the propagation of inherent bias errors, B_{IUT}, and precision errors generated during the calibration test, S_{IUT}, as defined in Equation 16. Bias errors (Type B) are primarily from the data acquisition system. Precision errors (Type A) are accounted for in the standard deviation of anemometer output reading during the duration of the data collection. Again, the value of t for 95% confidence at ∞ degrees of freedom is 1.96.

$$U_{IUT} = \sqrt{B_{IUT}^2 + (tS_{IUT})^2} \tag{16}$$

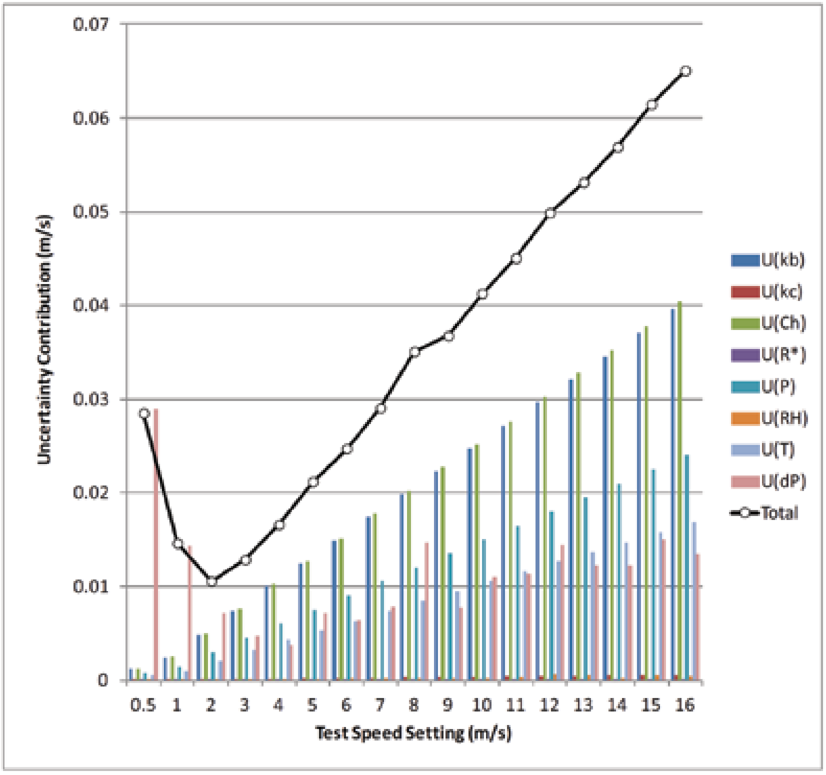

Figure 7. Uncertainty contributions from each dependent variable.

Uncertainty contribution from the degree of linearity between the test wind sensor output and the reference wind speed, U_{LR}, is determined by the variability in the wind speed residual at each test point. Using the resulting linear regression equation from the calibration table of test sensor output and reference wind speed, a calculated wind speed is determined with each measured test sensor output. The difference between this calculated speed and the reference wind speed is considered the wind speed residual. Thus, the uncertainty due to linearity is defined as follows:

$$U_{LR} = \sqrt{(tV_{res})^2} \quad . \qquad (17)$$

By combining the uncertainty in the reference wind speed, U_V, the uncertainty in the test sensor output, U_{IUT}, and the uncertainty due to linearity, U_{LR}, the uncertainty in the calibration test is then defined as follows:

$$U_{cal} = \sqrt{(U_V)^2 + (U_{IUT})^2 + (U_{LR})^2} \quad . \qquad (18)$$

Figure 8 displays the contributions to the overall uncertainty in the calibration of a Model C3 anemometer in ASWT1. Overall, the greatest contribution comes from the output of the test sensor, specifically from the increased randomness at the higher test speeds.

Conclusion

In summary, quality wind sensor calibrations are best performed in a controlled, uniform flow, low-turbulence wind tunnel as defined by test standards. To qualify a wind tunnel for wind sensor calibration testing, certain base performance features are to be surveyed and their requirements met. In addition, the qualification of a wind tunnel to perform wind sensor calibrations shall also include: 1) an evaluation of blockage due to the presence of the test sensor, 2) the repeatability of a reference sensor, and 3) interlaboratory comparisons with other similar facilities. Through a preliminary rigorous investigation, results from performance tests done so far for the Aero-Subsonic Wind Tunnel (ASWT1) at Bryza Wind Lab has shown to have met the facility requirements defined by test standards. Future investigation is still needed to identify a more accurate turbulence level, and continuous investigation is needed for the qualification of calibrating specific model sensors. Repeatability tests and one interlaboratory comparison show that calibration testing for the Model C3 anemometer is feasible in ASWT, where the estimated uncertainty ranges from 0.07 to 0.21 m/s for the calibration test range of 4 to 16 m/s. For further verification, additional interlaboratory comparisons is required.

References

[1] AIAA R-093-2003 (2003). Calibration of Subsonic and Transonic Wind Tunnels. American Institute of Astronautics and Aeronautics (AIAA).

[2] AIAA S-071A-1999 (1999). Assessment of experimental uncertainty with application to wind tunnel testing. American Institute of Astronautics and Aeronautics (AIAA).

[3] ASTM D 5096-02 (2002). Standard test method for determining the performance of a cup anemometer or propeller anemometer. American Society for Testing and Materials (ASTM).

[4] ASTM D 6011-96 (2008). Stan-

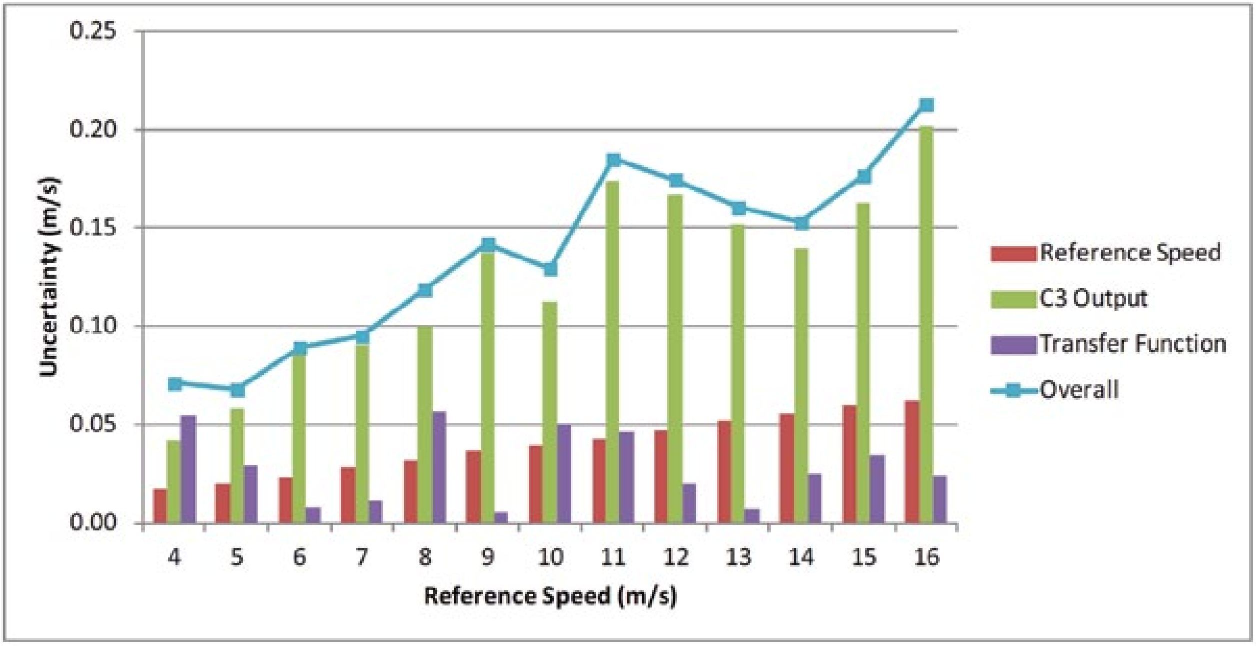

Figure 8. Contributions to the overall calibration uncertainty of a Model C3 anemometer in ASWT1.

dard test method for determining the performance of a sonic anemometer/thermometer. American Society for Testing and Materials (ASTM).

[5] IEC 61400-12-1, 1st ed. (2005). Wind turbines – Part 12-1: Power performance measurements of electricity producing wind turbines. International Electrotechnical Commission (IEC).

[6] ISO 17713-1 (2007). Meteorology – Wind measurements Part 1: Wind tunnel test methods for rotating anemometer performance. International Organization for Standardization (ISO).

[7] ISO 16622 (2002). Meteorology – Sonic anemometers/thermometers – Acceptance test methods for mean wind measurements. International Organization for Standardization (ISO).

[8] ISO/IEC Guide 98-3 (2008). Uncertainty of Measurement Part 3: Guide to the Expression of Uncertainty in Measurement (GUM:1995). International Organization for Standardization (ISO) and International Electrotechnical Commission (IEC).

[9] Coleman, H.W. and W.G. Steele, Jr. (2009). *Experimentation and Uncertainty Analysis for Engineers*, 3rd ed. John Wiley & Sons, Inc, New York, NY.

[10] Eecen, P.J. and M. de Noord (2005). ECN-C-05-66, Uncertainties in cup anemometer calibrations: Type A and Type B uncertainties. Energy Research Center of the Netherlands.

[11] Taylor, B.N. and C.E. Kuyatt (1994). NIST Technical Note 1297: Guidelines for Evaluating and Expressing the Uncertainty of NIST Measurement Results. National Institute for Standards and Technology.

Rachael V. Coquilla, President, Bryza Wind Lab, rvcoquilla@bryzawindlab.com.

Bryza Wind Lab is a company that specializes in wind tunnel test and consulting services including accredited wind sensor calibrations, laboratory instrumentation setup, custom experiments, and data analysis. Bryza's wind tunnel laboratory was established in Fairfield, California, USA, minutes from the Shiloh Wind Power Plant located in the Montezuma Hills of Solano County. www.bryzawindlab.com.

This paper was previously presented at the Measurement Science Conference (MSC), Anaheim, California, March 19-23, 2012. www.msc-conf.com.

Learning to Apply Metrology Principles to the Measurement of X-ray Intensities in the 500 eV to 110 keV Energy Range

Michael J. Haugh, Travis Pond, Christopher Silbernagel,
Peter Torres, Kent Marlett, Fletcher Goldin, Susan Cyr
National Security Technologies, LLC

1. Introduction

National Security Technologies, LLC (NSTec), Livermore Operations, has two optical radiation calibration laboratories accredited by the National Institute of Standards and Technology (NIST), and is now working towards accreditation for its X-ray laboratories. NSTec operates several laboratories with X-ray sources that generate X-rays in the energy range from 50 eV to 115 keV. These X-ray sources are used to characterize and calibrate diagnostics and diagnostic components used by the various national laboratories, particularly for plasma analysis on the Lawrence Livermore National Laboratory (LLNL) National Ignition Facility (NIF). Because X-ray photon flux measurement methods that can be accredited, i.e., traceable to NIST, have not been developed for sources operating in these energy ranges, NSTec, NIST, and the National Voluntary Accreditation Program (NVLAP) together have defined a path toward the development and validation of accredited metrology methods for X-ray energies. The methodology developed for the high energy X-ray (HEX) Laboratory was NSTec's starting point for X-ray metrology accreditation and will be the basis for the accredited processes in the other X-ray laboratories. This paper will serve as a teaching tool, by way of this example using the NSTec X-ray sources, for the process and methods used in developing an accredited traceable metrology.

NSTec's initial focus for accreditation of an X-ray source is on the HEX Lab. The HEX operates in the energy range from 8 keV to 115 keV, and is used to calibrate diagnostics that measure energy spectra, relative transmission, and absolute sensitivities. Two metrology methods are employed for HEX detector calibration. One metrology method employs radioactive nuclide sources with a traceable radioactive decay rate. The second method uses a photodiode detector calibrated at a synchrotron facility. Both methods will be discussed.

The energy dispersive radiation detectors used in the HEX Lab are calibrated using radionuclide sources. A number of crucial parameters, such as relative size between detector and radionuclide source, distances, decay rate uncertainties, etc. can introduce errors in the calibration, so a major effort for the procedure has been to quantify the total error. This effort will be described in detail.

2. X-Ray Sources at NSTec

2.1 Overview

There are three X-ray sources that are now operating at NSTec covering the X-ray spectral energy range from 500 eV to 110 keV. All the primary X-ray sources are the diode type; electrons are emitted from a heated tungsten filament, and then accelerated by an electric field to strike an anode. Two NSTec sources use a secondary beam that is generated when the primary beam strikes a sheet of material that fluoresces.

The diode source produces spectral lines that are characteristic of the anode material and a broad spectrum of radiation known as bremsstrahlung, peaking near one-

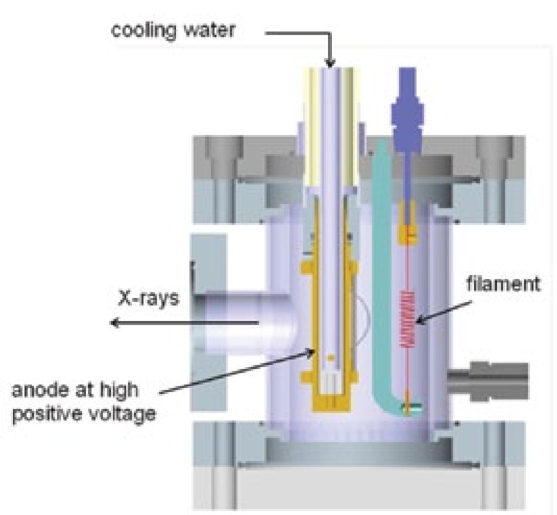

Figure1. Example of an X-ray diode.

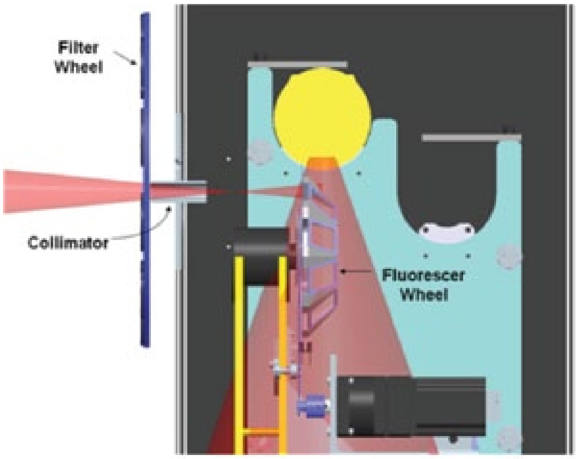

Figure 2. HEX source component, fluorescer and filter.

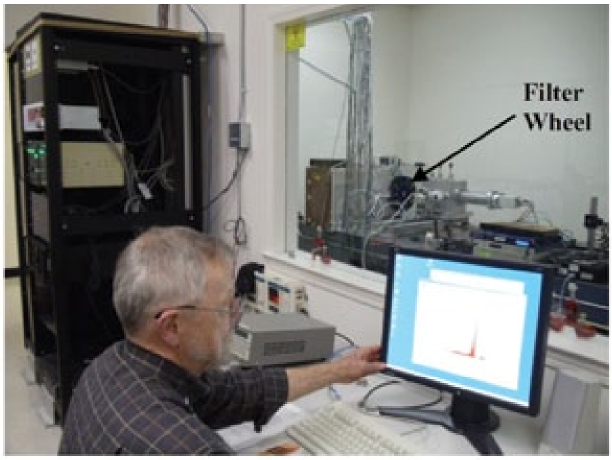

Figure 3. Remote adjustment of arrangement.

third of the accelerating voltage. A typical diode source is shown in Figure 1. The filament is heated by an independent electrical circuit that is near ground potential. The anode is maintained at a high positive voltage so that the electrons emitted from the filament are accelerated and strike the anode at the energy determined by the voltage difference. The electric field is shaped using guide wires. X-rays are emitted in all directions and some exit the aperture, as shown in Figure 1, and enter into the sample chamber. The anode is water-cooled so that a high beam current can be tolerated, thus giving a strong X-ray intensity. This intensity allows collimation of the X-ray beam with a pair of slits, as well as isolation of individual spectral lines using a diffraction crystal. The narrow band X-ray source can measure sample properties such as filter transmission, crystal reflectivity, and sensor efficiency. The source and sample chamber are in vacuum. The voltage supply is 20 kV, making the highest available spectral line nearly 17 keV (*Zr* K spectral lines).

The other diode source uses anodes that are cooled only by thermal conduction through the mechanical connections. This limits its operation to 10 W and 10 kV, with a usable spectral range from 700 eV to 8400 eV. It is often used to measure the absolute efficiency of X-ray cameras and the sensitivity variation across the sensor pixels.

The third source covers the spectral energy range from 8 keV to 111 keV and uses fluorescence to generate X-rays. This source is progressing toward NIST accreditation and will be described in detail in the next section. The fourth source is currently being built and will cover the X-ray spectral region from 50 eV to several keV and also operates in the fluorescer principle.

The NSTec X-ray sources are used to calibrate and characterize components or complete systems that are used in the study of plasmas and similar efforts. A large component of our present calibration efforts is for diagnostics that are used on the NIF target diagnostics.

2.2 The HEX Source

The HEX generates spectral lines in a beam using a commercial 160 kV tungsten X-ray tube and the fluorescing targets that are enclosed in a lead box. An exit collimator in the lead box shapes the X-ray beam. The arrangement of the components is shown in Figure 2.

The end of the commercial X-ray tube is shown in yellow. The pink trapezoid that starts at the tube represents the primary X-ray beam. The fluorescers are mounted on the motorized wheel in the rectangles shown on the wheel. The fluorescer emits in all directions, but the X-ray beam is defined by the collimator inserted into the wall of the lead box, and the beam path is illustrated by the pink triangles. There is a filter wheel mounted downstream from the collimator, and it is also motorized. The fluorescer and the filter can be set from the computer in an adjacent control room, as shown in Figure 3. The fluorescer is usually a thin sheet made of elemental metal, but metal compounds are sometimes used. The maximum intensities obtained when an 11.5 mm diameter collimator is used are on the order of 1×10^6 photons per cm^2 per second, at one meter from the fluorescer, depending on the fluorescer material. The spectral lines used range from 8 keV to 115 keV.

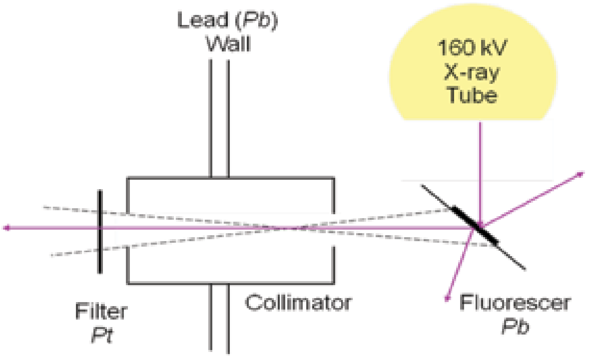

Figure 4. Illustration of fluorescence principle.

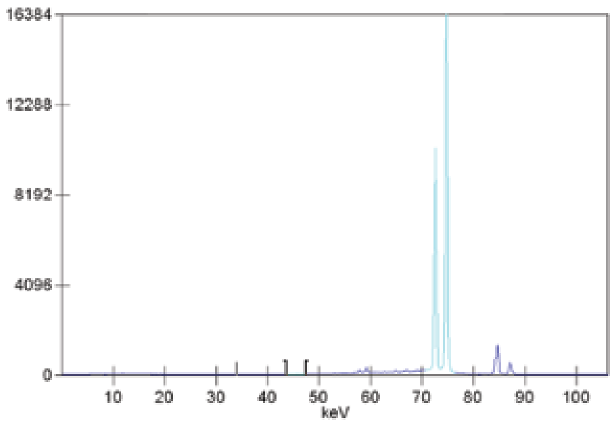

Figure 5. Pb Spectrum, Pt Filter.

The fluorescer operation is illustrated by Figure 4. For this example, the fluorescing material is a thin lead (*Pb*) sheet, with a thickness of approximately 250 µm, and the filter is a thin platinum (*Pt*) sheet. Table 1 gives the properties of the fluorescer and filter. The high energy X-ray lines are transmitted by the filter but the low energy lines are stopped by the filter.

Filter	Fluorescer
Platinum (*Pt*), 50 µm thick	Lead (*Pb*)
Transmission	Spectral Lines, keV
0.72	75, 73
0.40	85
2 x 10^{-5}	10.6, 10.4, 12.6, 14.8
0	2.3

Table 1. X-ray Fluorescence.

This method provides a reasonably narrow spectral energy that can be used to calibrate detectors at a range of well defined energies. The resulting spectrum from the arrangement is shown in Figure 5.

The HEX source sits at the end of an optical table as shown in Figure 6. The sample and the detectors are mounted on the optical table. The control room is separated from the HEX laboratory, as seen in Figure 3.

2.3 Applications

The HEX has been used to calibrate the filters and fluorescer metal sheets that are used to isolate X-ray energy bands in the NIF FFLEX (Filter Fluorescer Experiment) diagnostic. The FFLEX produces information about the spectral distribution of X-ray flux at the higher X-ray energies. A goal is to estimate the temperature of hot electrons. Calibration is done by measuring the X-ray flux with an energy dispersive X-ray detector, both with the filter in the beam and with the filter removed from the beam. A typical calibration result using gold (*Au*) as the filter material is shown in Figure 7.

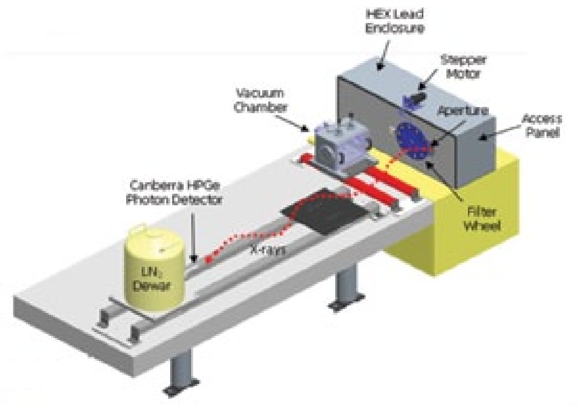

Figure 6. HEX layout.

The transmission of the *Au* filter is measured as a function of energy at multiple locations on the filter and then, using literature data [1] for the X-ray transmission of that material, the filter thickness that best fits the data is determined.

Another application for the FFLEX diagnostic was to measure the sensitivity of a scintillator / photomultiplier tube (PMT) combination at energies near 100 keV. For this type of calibration, a well defined X-ray beam was produced by using a long tungsten collimator. The output current from the scintillator/PMT was measured when mounted after the collimator. The scintillator / PMT was removed from the X-ray beam and the X-ray flux was measured using an energy dispersive detector. This application is an absolute measurement, thus imposing a much more stringent requirement on the detector accuracy than the relative measurement described in the first application.

Other applications require knowing the absolute X-ray intensities, as in camera sensitivity measurement. Calibrations have been done for both Charge Coupled Device (CCD) cameras and Charge Injection Device (CID) cameras. As an example, an imaging device was needed as part of a spectrograph that observed the NIF implosion at several X-ray ranges. A CID camera was planned for the measurement, and the camera performance was modeled using the device structure information and a few assumptions. Then the camera output count per photon was measured using the HEX at several X-ray energies. Quantitative accuracy was critical to the application. The HEX was used to calibrate absolutely the image plate X-ray intensity accuracy over an energy range from 10 keV to 80 keV.

The X-ray beam was characterized geometrically using image plates to optimize collimator and distance choices. The intensity distribution was measured using the energy dispersive detector. Multiple images were taken with the CID, and then the detector was placed at the same location

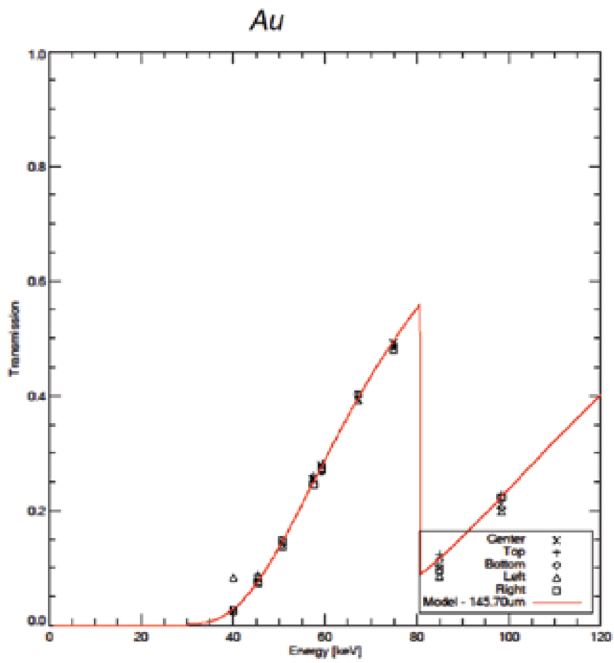

Figure 7. HEX filter calibration summary. Material: Au Nominal Thickness: 141.4 µm. Model Thickness: 145.70 µm.

as the center of the CID had been located. The results are shown in Figure 8. The camera response was measured for two CID cameras at three spectral energies over the range of interest. A comparison using alterations in the model's thickness parameter is shown by the continuous lines. The 7µm thickness was the vendor's specification.

3. X-Ray Detectors

3.1 Solid State Detectors

The detectors used with the NSTec sources are based on semiconductor active materials such as *Si*, *Ge*, and *CdTe*. One type of detector measures total power in the X-ray beam per unit area. A second type is energy dispersive, producing an energy spectrum. The energy dispersive detector uses the pulses of electron-hole pairs that are produced by the X-ray photon. These pulses are amplified, and then binned according to pulse height, which is proportional to the photon energy. An energy spectrum is thus produced. The total flux detector produces a current that is proportional to the total number of electron-hole pairs that are produced by the interaction of the X-ray photon with the semiconductor sensor. For this work with the HEX source, the *Ge* and *CdTe* sensors were used as energy dispersive detectors and the *Si* sensor was used for total flux measurement. See Knoll's book [2] on radiation detection and measurement.

3.2 Solid State Semiconductor Energy Dispersive Detectors

The X-ray photon interacts with the semiconductor material, primarily through the photoelectric effect, to produce electron-hole pairs. The number of electron-hole pairs is proportional to the energy of the X-ray photon. In general it takes several eV to produce an electron-hole pair, the exact energy depending on the semiconductor material. A bias voltage is applied to the semiconductor and the electric fields generated require cooling of the detector. The voltage pulses produced by an individual X-rays are amplified and then counted according to pulse height. Pulses that have heights within a certain range are

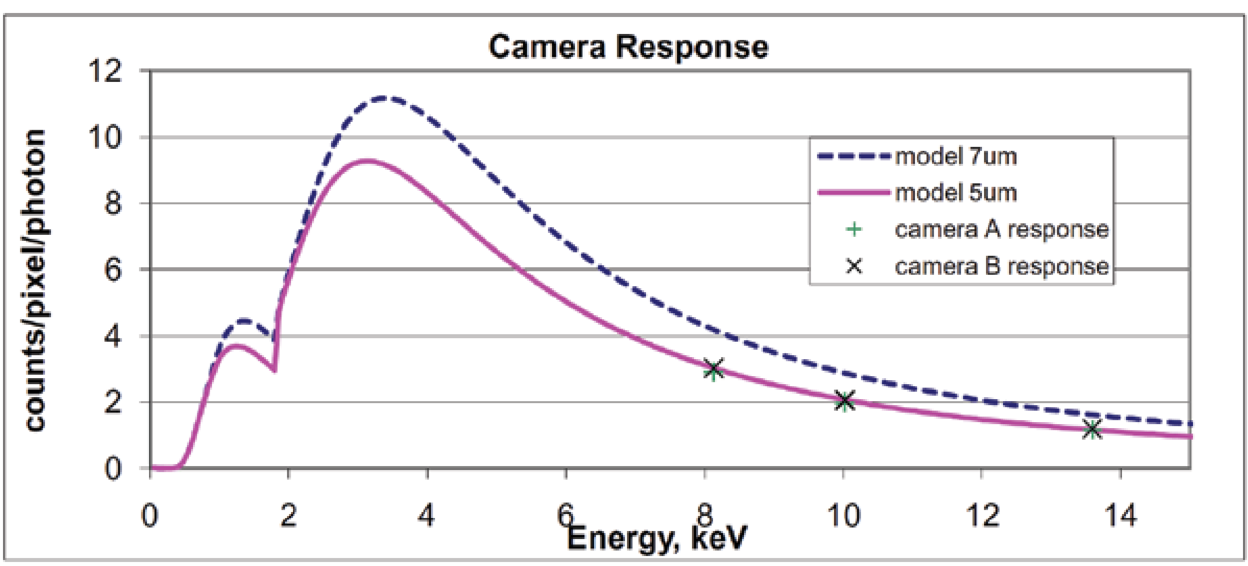

Figure 8. Camera response, intensity distribution.

effectively assigned to channels according to the average pulse height by a processor referred to as a multi-channel analyzer. This produces an energy spectrum of the photons in the X-ray beam that is intersected by the detector. The resolving power of the energy dispersive detector is generally limited to several hundred eV.

The detector sensitivity falls off at lower energies due to absorption at the front surface by a "dead" layer of the sensor. It falls off at higher energies the photons begin to be transmitted by the sensor. The *Ge* and *CdTe* detectors are designed to operate optimally in the 10 keV to slightly over 100 keV. The X-ray photon interacts with the sensor material in ways other than forming electron-hole pairs, which can reduce its sensitivity. If a photon has sufficient energy, it can knock out a 1s electron of the sensor material, a higher state electron can transition down into the 1s vacancy. A second photon having an energy equal to the energy between these two states can then be emitted. The sensor then produces a corresponding pulse of electron-hole pairs that is smaller than the base peak by the energy difference between the incoming X-ray photon and the binding energy of the sensor material 1s electron. This is referred to as an escape peak, and effectively that incoming X-ray photon is not counted. There are other losses that are produced by the detector fabrication details.

The *Ge* detector uses a high purity *Ge* disk, 8 mm diameter and 5 mm thick, that is cooled to liquid nitrogen temperature. The sensor is in a vacuum chamber that has a 4 mil thick beryllium (*Be*) window for X-ray beam entry. *Ge* has an escape peak near 11.1 keV. Figure 9 shows a spectrum from the radioactive isotope of americium having an atomic mass of 241 (*Am*-241). This source emits gamma radiation (X-rays that are produced by nuclear transitions) at 59.5 keV and 26.4 keV and X-rays that are produced by electronic transitions from the *Am* decay daughter neptunium (*Np*) ion are seen in the 13 keV to 22 keV range. A small escape peak is seen near 49 keV and a larger escape peak is seen near 8 keV. The *CdTe* sensor is a 5 mm square that is 1 mm thick. It is cooled sufficiently using a thermoelectric cooler so that a 400 V bias voltage can be applied without electrical breakdown. It also operates in vacuum with a 4 mm *Be* window. The energy required to form an electron-hole pair for this material is 4.43 eV [3]. Escape peaks occur near 27 keV and 32 keV. Electron-hole pairs formed near the back contact of the detector cause fluctuations in pulse height and they are not seen as belonging to the true peak. This is a loss in sensitivity. The *Am*-241 spectrum for the *CdTe* detector is given in Figure 10. Note that there are several peaks in the 30 keV to 40 keV energy range that are not in the spectrum when the *Ge* sensor is used. These are related to the escape peaks for *CdTe*.

3.3 Photodiodes for Intensity Measurements

Si photodiodes are used with all of the NSTec X-ray sources to measure the X-ray beam intensity. These devices measure the total current produced by the hole-pairs generated by the interaction of the X-ray photons with the *Si*. The energy needed to form a hole-electron pair in high purity *Si* is 3.63eV. The detectors are designed to have minimum surface dead layer so that they are accurate down to 1 keV. Representative samples of these diodes have been calibrated at the Physikalische-Technische Bundestalt synchrotron in Germany for the energy range from 1 keV to 60 keV [4]. Calibrations in the range of 50 eV to 60 keV are also being planned.

4. Detector Calibration

4.1 The Concept: Using Radioactive Sources

Radioactive sources provide a variety of spectral lines at well defined energies, as was described in the energy dispersive detector section (section 3.2). The photon output is directly proportional to the activity of the radioactive source, and the activity measurement is traceable to NIST. The uncertainty for the activity is provided by the vendor.

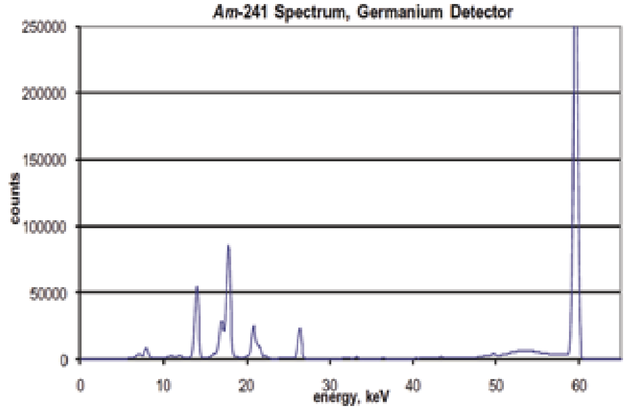

Figure 9. *Am*-241 spectrum, *Ge* detector.

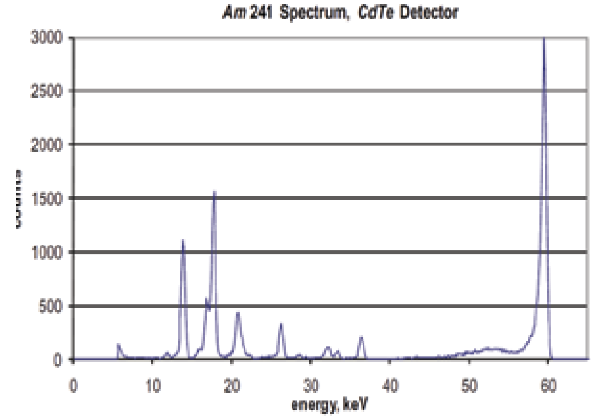

Figure10. *Am*-241 spectrum, *CdTe* detector.

The activity R at time t is given by:

$$R = R_0 e^{-(t \ln 2)/\tau},$$

where R_0 is activity at time t=0 and τ is the radionuclide half life.

The radioactive source is placed at some distance from the detector chosen sufficiently large so that the sizes of the source and detector elements are negligible in comparison. The power Ω at the detector in photons per second for a selected spectral band is given by:

$$\Omega = R\ B\ (A_d/4\ \pi r^2)\ T,$$

where B is branching ratio; A_d is detector area; r is the distance between radioactive source and the detector; and T is X-ray transmittance through r cm of air.

The branching ratio is the fraction of nuclear decays that produce the selected spectral band. It has an experimental uncertainty associated with the measurement of that property. If the activity was measured using a gamma emission, the uncertainty is reduced to that of this measurement itself and is given with the radionuclide NIST traceable certification.

The detector efficiency η, is then given by:

$$\eta = S/\Omega,$$

where S is the photon count measured by the detector.

The measurement arrangement is shown in Figure 11 in which the *Ge* detector is seen on the right side and the detector window faces the radioactive source. An optical distance meter is located at the far left of the optical rail and is also at the same height as the source and detector and measures the distance from the radioactive source and to the detector window. The internal distances for source and detector are provided by the manufacturers to an accuracy of 0.5 mm or better. The distance sensor has an accuracy of ±1 mm and was calibrated at NIST within a month of the detector calibration measurements. Thus the source-to-detector distance accuracy is ±1 mm.

Figure 11. Experimental arrangement for calibrating detectors using radionuclides

Spectral Energy, keV	Spectral Type	Radionuclide
5.97	Mn, K line	Fe55
22.16	Ag, K line	Cd109
26.34		Am241
41.3	Eu, K line	Gd153
59.54		Am241
88.00		Cd109
97.43		Gd153
103.18		Gd153

Table 2. Spectral Lines Used for the Calibration of the Ge and CdTe Detectors.

4.2 Measurement Results

Measurement results using the methods described previously are given in this section. The spectral lines that were used for these measurements are given in Table 2.

Efficiency measurements for the *Ge* detector are shown in Figure 12.

The measurements for the *CdTe* detector quantum efficiency are shown in Figure 13. These measurements show a precision near 3% at the 95% confidence level. The *Ge* detector shows a peak efficiency near 60KeV and falls off in efficiency at lower and higher spectral energies. The *CdTe* detector has a peak efficiency near 30 keV and also falls off in efficiency at lower and higher spectral energies.

In Figures 10 and 11, note the large gaps that exist between the points. It has been described earlier that escape peaks occur above the K edges (minimum energy needed to remove a *1s* electron) of the detector materials, and this reduces the detector efficiency. This effect has been directly observed in calibration of a *Si* photodiode in the vicinity of the *Si* K edge (1.39keV) [4]. The K edges for *Ge*, *Cd*, and *Te* are 11.1 keV, 26.71 keV, and 31.81 keV respectively [5]. The situation regarding the large gaps can be improved by using more radionuclides but there are availability and economic restrictions that will limit this approach. We plan to fill in the gaps to fill in these energy gaps by calibrating an *Si* detector up to 60 keV using a synchrotron. This calibration can then be transferred to the other detectors using the HEX source.

5. NVLAP Accreditation Procedure

Until NSTec, NIST, and NVLAP collaborated on the accreditation of the methodology for calibrating X-ray intensity rather than dosimetry,

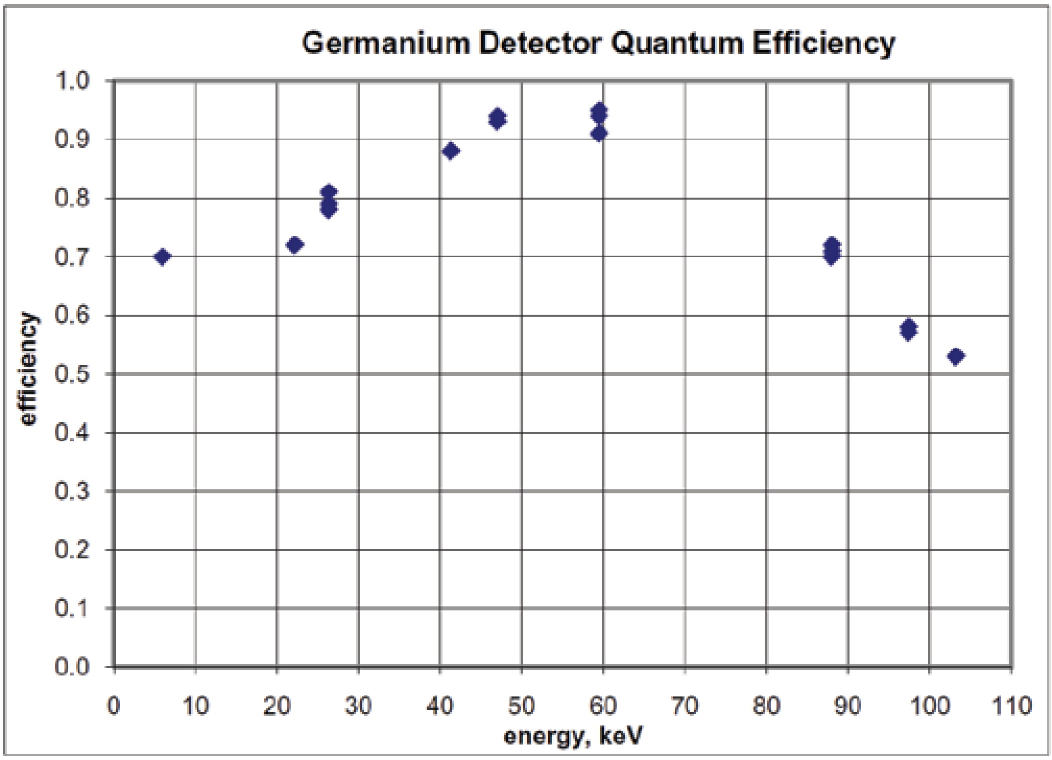

Figure 12. Measurements of the Ge detector quantum efficiency using the radionuclide sources.

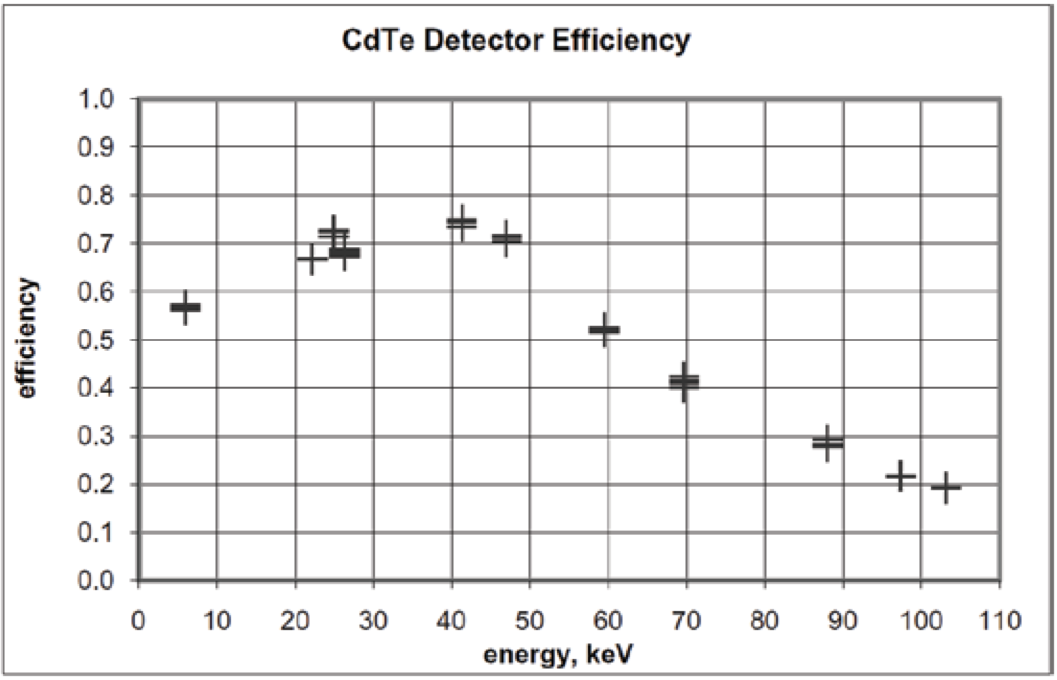

Figure 13. Measurements of the CdTe detector quantum efficiency using radionuclide sources.

1	Radionuclide signal measurement reproducibility.
2	Radionuclide activity.
3	Radionuclide branching ratio, when needed; daughter X-ray emission.
4	Distance measurement, source to detector.
5	Detector size.
6	Measurement duration.
7	Choice of region of interest (ROI) for counting photons belonging to a spectral line.
8	Radionuclide decay rate.
9	Energy accuracy.
10	Air transmission of the X-ray.
11	Curve fit to points between the measured points.

Table 3. Quantities in the Calibration Procedure Contributing to the Overall Uncertainty.

calibration methods in the high energy X-ray realm anywhere were neither traceable nor repeatable. Through the development of an accredited methodology for experiments in this high energy realm, the diagnostics and system components for pulsed high energy physics experiments conducted at the national laboratories such as LLNL can now be calibrated correctly. Since the NSTec High Energy Density Physics (HEDP) group had already passed the NVLAP accreditation process on specific measurements in two laser laboratories, the accreditation for the HEX Lab was much simpler. The required rigor of the quality assurance management system is already in place and approved. The required steps for accreditation are:

1. Determination of customer requirements
2. Development of calibration procedures and documentation of the procedures
3. Traceability
4. Evaluation of measurement reproducibility
5. Determination of uncertainty
6. Generation of calibration certificates.

The main customer requirement is to have the capability to calibrate customer detectors and components to an absolute value with known uncertainties.

The previous sections have described the detector calibration procedure which is then used to calibrate our X-ray source. The radionuclides used are traceable to NIST, and the vendor of these radionuclides participates in a measurement assurance program with NIST. NIST regularly sends to the vendor standard radionuclide sources with activity that is unknown to the vendor who then measures the activity and submits the results back to NIST. NIST then checks the measurements to verify that they meet the required accuracy. The distance measurement traceability was described earlier.

As with all traceable measurements, repeatability is the primary condition required for accreditation. The variation in repeated measurements quantifies random errors. Only when calibrations using a common procedure and equipment produce the results that vary within an acceptable range, even with different operators, is the technical process is ready for NVLAP review.

Initial evaluation of measurement repeatability was described in the measurement section. We are in the process of evaluating the overall uncertainty. A list of the factors being considered is given in Table 3.

6. Conclusion

This paper describes the development of a procedure to produce a traceable calibration of X-ray detectors that are then used to calibrate the X-ray sources. This provides a traceable method for calibrating X-ray detectors and components for customers. There are still several steps that will be done in the next few months to complete the accreditation procedure. This includes the calibration of an *Si* photodiode at a synchrotron that is NIST approved up to 60 keV so that the detector efficiency in the spectral gaps between radionuclide lines can be measured. Then we will determine the numerical values for the uncertainties listed in Table 3. And finally, we will request approval of the procedures and documentation by the NVLAP assessment representatives.

References

[1] "NIST: X-Ray Mass Attenuation Coefficients," http://www.nist.gov/pml/data/xraycoef/index.cfm.

[2] Knoll, G. F., *Radiation Detection and Measurement*, 3rd edition, John Wiley & Sons (2000).

[3] Quaranta, C., Canali, G., Ottavani, G., Zanio, K., "Electron-hole Pair Ionization Energy in CdTe between 85K and 350K," *Lettere Al Nuovo Cimento*, 4, p. 908-910 (1969).

[4] "PTB Measurement Results for a AXUV100GX Photodiode" http://www.ird-inc.com/xray/data/PTB_Measurement_Data.txt.

[5] Gullikson, E., "CXRO X-Ray Interactions With Matter," http://henke.lbl.gov/optical_constants/.

Michael J. Haugh, Travis Pond, Christopher Silbernagel, Peter Torres, Kent Marlett, Fletcher Goldin, and Susan Cyr, National Security Technologies, LLC, 161 S. Vasco Rd. Suite A, Livermore CA 94550.

This paper was previously presented at the Measurement Science Conference (MSC) in Pasadena, California, March 15-18, 2011. www.msc-conf.com.

CLASSIFIEDS

METROLOGY
restor™

World-Class
Calibration Excellence

When compliance matters, trust Restor to deliver test equipment calibration and repair services quickly and with no compromise on quality. With Restor, your critical equipment will be calibrated right; Certificates and datasheets will meet stringent standards and pass audit. Save time and money over the OEMs.

- A2LA accredited for calibration ISO 17025, ANSI Z540.3 & Z540-1
- DC to 50 GHz Capability
- EMI Receivers IAW CISPR 16-1-1
- LISN's IAW CISPR 16-1-2, RTCA DO-160 & MIL STD 461
- CDN's & ISN's IAW IEC 61000-4-6 & CISPR 22
- ESD Simulators & Guns IAW 61000-4-2:2008
- EFT, Burst & Surge Generators

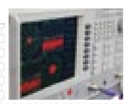

Get a no-obligation "Quick Quote" at:
www.restormetrology.com
or call: **877-220-5554**

CAL-TOONS **by Ted Green** teddytoons@verizon.net

OKAY. WELL, SOME METROLOGISTS HAVE MORE FUN THAN OTHERS.*

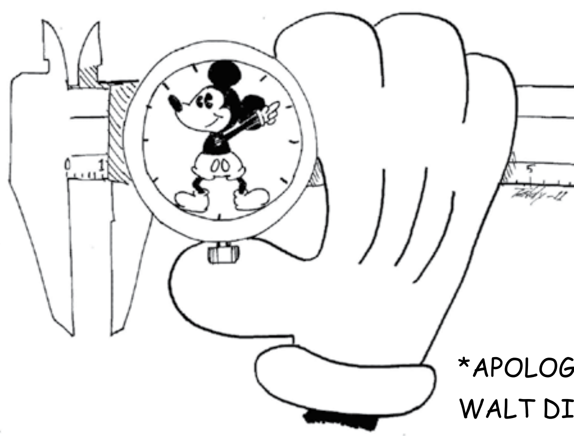

*APOLOGIES TO WALT DISNEY

Equipment Reliability Institute

Sept 11-13, 2012 - **Seismic Protection of Critical Equipment**, Acton, MA

Oct 15-17, 2012 - **Fundamentals of Vibration and Shock Testing with emphasis on Fixture Design**, Sunnyvale, CA

For more dates & locations, visit: ***www.equipment-reliability.com***.

METROLOGY BOOKS FOR SALE

A Paperless Calibration Department That Meets Biotech, Pharmaceutical & Medical Device Requirements
by Jay L. Bucher

Paperless Calibration Compliance For National & International Standards & Regulations
by Jay L. Bucher

Available in Spiral/Hardbound binding for $139.95/$169.95, plus shipping.

Purchase online:
http://www.callabmag.com/?page_id=1828.

Now Available
16 Years of
Cal Lab Magazine
on DVD
1995-2010
$195
Order now at
303-317-5295
or order online at
www.callabmag.com
under "Products"

PDF Format

DISCOVER THE "BLUE BOX" DIFFERENCE™

Model MI9060 Precision Thermometer

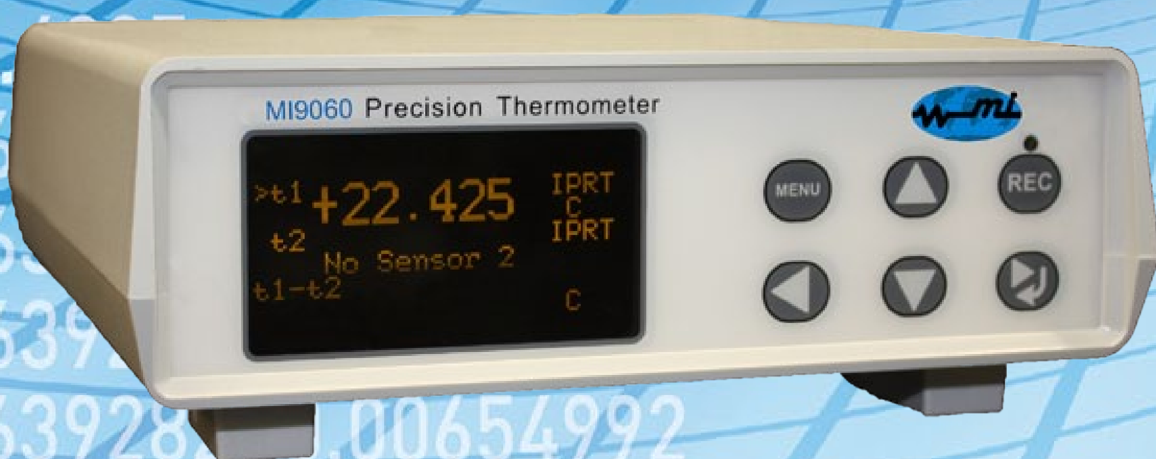

- Accuracy ±0.01°C
- Resolution 0.001°C
- Dual Channels
- Range -200°C to 850°C
- Data Storage to USB
- Wireless Data Transfer

Measurements International
Metrology is Our Science, Accuracy is Our Business™

Corporate Headquarters

Measurements International
PO Box 2359, 118 Commerce Drive
Prescott, Ontario, Canada K0E 1T0

Phone: (613) 925-5934
Fax: (613) 925-1195
Email: sales@mintl.com
Toll Free: 1-800-324-4988

Worldwide Offices

MI-USA
Phone: (407) 706-0328
Fax: (407) 706-0318
Email: sales@mintl.com

Toll Free: 1-866-684-6393

MI-China
Phone: 86-10-64459890
Fax: 86-10-64459871
Email: sales@mintl.com

MI-Europe
Phone: (420) 731-440-663
Fax: (420) 572-572-358
Email: sales@mintl.com

www.mintl.com